

Cas12a2 elicits abortive infection via RNA-triggered destruction of double-stranded DNA

Oleg Dmytrenko¹, Gina C. Neumann², Thomson Hallmark³, Dylan J. Keiser³, Valerie M. Crowley³,
Elena Vialeto¹, Ioannis Mougiakos¹, Katharina G. Wandera¹, Hannah Domgaard³, Johannes
Weber¹, Josie Metcalf³, Matthew B. Begemann², Benjamin N. Gray^{2*}, Ryan N. Jackson^{3*}, Chase
L. Beisel^{1,4*}

¹Helmholtz Institute for RNA-based Infection Research, Helmholtz Centre for Infection
Research, Würzburg, Germany

²Benson Hill Inc., St. Louis, Missouri USA

³Department of Chemistry and Biochemistry, Utah State University, Logan Utah, USA

⁴Medical faculty, University of Würzburg, Würzburg, Germany

Correspondence: bgray@bensonhill.com (to B.N.G.), ryan.jackson@usu.edu (to R.N.J.), and
chase.beisel@helmholtz-hiri.de (to C.L.B.)

1 ABSTRACT

2 Bacterial abortive infection systems limit the spread of foreign invaders by shutting down or killing
3 infected cells before the invaders can replicate^{1,2}. Several RNA-targeting CRISPR-Cas systems
4 (e.g., types III and VI) cause Abi phenotypes by activating indiscriminate RNases^{3–5}. However, a
5 CRISPR-mediated abortive mechanism that relies on indiscriminate DNase activity has yet to be
6 observed. Here we report that RNA targeting by the type V Cas12a2 nuclease drives abortive
7 infection through non-specific cleavage of double-stranded (ds)DNA. Upon recognition of an RNA
8 target with an activating protospacer-flanking sequence, Cas12a2 efficiently degrades single-
9 stranded (ss)RNA, ssDNA, and dsDNA. Within cells, the dsDNase activity induces an SOS
10 response and impairs growth, stemming the infection. Finally, we harnessed the collateral activity
11 of Cas12a2 for direct RNA detection, demonstrating that Cas12a2 can be repurposed as an RNA-
12 guided, RNA-targeting tool. These findings expand the known defensive capabilities of CRISPR-
13 Cas systems and create additional opportunities for CRISPR technologies.

14 **MAIN TEXT**

15 All forms of life employ defense strategies that cause cells to go dormant or die to limit the spread
16 of infectious agents¹. In bacteria and archaea, this strategy is called Abortive infection (Abi), and
17 it is used by a vast variety of bacterial defense systems^{1,2}. Recently, it was shown that CRISPR
18 RNA (crRNA)-guided adaptive immune systems that target RNA cause Abi phenotypes³⁻⁶. In type
19 III systems, target RNA binding triggers production of cyclic oligoadenylate secondary
20 messengers that in turn activate indiscriminate accessory RNases (e.g., Cms6/Csx1)^{4,5,7-9}. Type
21 VI systems also non-specifically degrade RNA, but instead of relying on a secondary messenger
22 and an accessory protein, the Cas13 single-effector nuclease acts as both crRNA-guided effector
23 and indiscriminate nuclease^{3,10,11}. In each case, the indiscriminate RNase activities cleave both
24 viral and host RNAs, reducing virus replication and causing cellular dormancy as an abortive
25 phenotype³⁻⁵. It has been proposed that CRISPR-mediated DNase activity may also cause Abi
26 through indiscriminate dsDNases (e.g., NucC) activated by type III system secondary
27 messengers^{12,13}, or indiscriminate ssDNase activity from type V Cas12a effectors¹⁴. However,
28 type III CRISPR-mediated dsDNase activity has yet to be examined *in vivo*, and the ssDNase
29 activity of Cas12a has not been shown to cause Abi¹⁵.

30

31 Here we reveal that Cas12a2, a type V single-effector CRISPR-associated (Cas) nuclease,
32 induces an Abi phenotype when challenged with plasmids complementary to crRNA-guides.
33 Biochemical assays with recombinant protein revealed that Cas12a2 recognizes RNA targets that
34 unleash non-specific dsDNA, single-stranded (ss)DNA, and ssRNA nuclease activities distinct
35 from those of other single-subunit RNA-targeting (e.g., Cas13a) and dsDNA-targeting (e.g.,
36 Cas12a) Cas nucleases^{11,16,17}. Additionally, we show that the Cas12a2 non-specific nuclease
37 activities damage bacterial DNA, triggering the SOS response and impairing cell growth.
38 Collectively these results suggest that the dsDNase activity of Cas12a2 is instrumental in
39 triggering the Abi phenotype. Additionally, as a proof-of-principle demonstration, we show that

40 Cas12a2 can detect RNA at a sensitivity comparable to that of RNA-targeting Cas13a nuclease
41 at various temperatures¹⁸.

42

43 **Cas12a2 targeting results in an abortive infection phenotype**

44 Cas12a2 is a type V effector nuclease previously grouped with Cas12a sequences¹⁶ and later
45 described as a Cas12a variant due to similarities in the CRISPR repeat sequence and the
46 presence of a homologous RuvC endonuclease domain¹⁹ (**Fig. 1a**). However, in our phylogenetic
47 analysis with additional orthologs, we found that Cas12a2 sequences form a distinct clade within
48 the type V phylogeny (**Fig. 1a and Extended Data Fig. 1**). Although Cas12a2 and Cas12a
49 possess related RuvC domains, Cas12a2 is distinguished from Cas12a by the presence of a large
50 domain of unknown function located in place of the Cas12a bridge helix as well as a zinc-finger
51 domain in place of the Cas12a Nuc domain (**Fig. 1b and Extended Data Fig. 2**). Considering
52 their original classification as well as our phylogenetic data and structural results²⁰, we named
53 these distinct type V nucleases Cas12a2.

54

55 Intriguingly, some CRISPR-Cas systems contain both *cas12a2* and *cas12a* genes in tandem next
56 to a shared CRISPR array (**Fig. 1c**). Considering that *cas12a* and *cas12a2* are adjacent to
57 CRISPR repeats with similar sequences (**Extended Data Fig. 3**) and that Cas12a2 is predicted
58 to be structurally similar throughout regions known in Cas12a to bind and process the crRNA¹⁹,
59 we hypothesized that both proteins bind and process similar crRNA guides. However, because
60 the proteins are diverse in other domains, we further hypothesized Cas12a2 performs a defense
61 function distinct from the dsDNA-targeting activity of Cas12a¹⁶.

62

63 To test these hypotheses, we transferred the *cas12a2* gene from the sulfur-oxidizing
64 epsilonproteobacterium *Sulfuricurvum* sp. PC08-66 (SuCas12a2) along with a CRISPR array on
65 an expression plasmid into *E. coli* cells. We then performed a traditional plasmid interference

66 assay that depletes cells by selecting for both the plasmid containing the nuclease and crRNA
67 and a target plasmid (**Fig. 1e**). This assay detects broad immune system activity but cannot
68 distinguish between defense activities that only deplete the target from those that activate Abi
69 phenotypes. To test if Cas12a2 utilizes an Abi mechanism, we modified the plasmid interference
70 assay to only deplete cells under Abi phenotypes by only selecting for the nuclease plasmid (**Fig.**
71 **1e**). Consistent with our hypothesis that Cas12a2 functions differently than Cas12a, Cas12a2
72 depleted cells in both the traditional (~1,900 fold reduction) and modified (~1,300 fold reduction)
73 plasmid interference assays with different targeting guides, while Cas12a from *Lachnospiraceae*
74 *bacterium* (LbCas12a) only depleted cells in the traditional assay (**Figs 1f**). Similar trends were
75 observed with different target sites, different Cas12a2 homologs, and when assessing the Cas12a
76 from *Prevotella bryantii* B14 (Pb2Cas12a) (**Extended Data Fig. 4**). Additionally, mutating
77 predicted active residues within any of the three RuvC motifs in SuCas12a2 eliminated immune
78 function (**Fig. 1g**). Collectively, these results indicated that Cas12a2 relies on a RuvC nuclease
79 domain and induces Abi with a mechanism distinct from that of Cas12a.

80
81

82 **RNA targeting by Cas12a2 triggers non-specific degradation of double-stranded DNA,
83 single-stranded DNA, and single-stranded RNA**

84 CRISPR systems that cause Abi phenotypes (e.g., types III and VI) rely on indiscriminate RNases
85 activated by RNA targeting³⁻⁵. To determine if Cas12a2 utilizes a similar mechanism, we
86 recombinantly expressed and purified SuCas12a2 and tested its enzymatic activities *in vitro* (**Fig.**
87 **2 and Extended Data Fig. 5**). However, before examining the nucleic acid targeting activities, we
88 needed to determine how Cas12a2 crRNAs are processed.

89

90 The CRISPR repeats of Cas12a and Cas12a2 systems are highly conserved on the 3' side
91 (**Extended Data Fig. 3**), and sequence alignments predict Cas12a2 shares secondary structure
92 in the region of the Cas12a pre-crRNA processing active site^{19,21} (**Extended Data Fig. 6**).

93 Consistent with this prediction, an RNA-processing assay coupled to RNA sequencing revealed
94 that SuCas12a2 processes its pre-crRNAs one nucleotide (nt) downstream of the position cleaved
95 by Cas12a. Mutating basic amino acids (K784 and R785) located in the predicted RNA processing
96 active site abolished activity²² (**Fig. 1c and Extended Data Fig. 7a-c**). Similar processing was
97 observed *in vivo* with co-expressed Cas12a2 and a single-spacer CRISPR array, producing ~42-
98 nt crRNAs with guide sequences ~24 nts long (**Extended Data Fig. 7d**). Furthermore, plasmid
99 interference assays revealed that Cas12a and Cas12a2 can interchange guides without impairing
100 immunity (**Extended Data Fig. 8**). Therefore, the Cas12a2 nuclease processes its own crRNA
101 guides like other type V effector nucleases^{21,23} and can share crRNAs with Cas12a.

102

103 To determine the nucleic-acid target preference of crRNA-guided Cas12a2, complementary
104 ssRNA, ssDNA, and dsDNA substrates containing an A/T-rich flanking sequence (paralleling
105 Cas12a substrates^{16,22}) was fluorescently labeled with a FAM molecule and combined with
106 crRNA-guided Cas12a2 (**Fig. 2a**). Similar to CRISPR-Cas systems that cause Abi, yet unlike the
107 dsDNA-targeting Cas12a, Cas12a2 is activated only in the presence of complementary RNA
108 targets. Additionally, this observation suggests that spurious transcription of our target plasmid is
109 sufficient to activate the immune system *in vivo* (**Fig. 1f**), consistent with what has been observed
110 with type III systems²⁴.

111

112 As other Cas Abi mechanisms rely on collateral indiscriminate RNase activity, we decided to
113 explore whether specific RNA targeting by Cas12a2 induces indiscriminate nuclease activity. We
114 found that SuCas12a2 robustly degraded FAM-labeled ssRNA, ssDNA and dsDNA substrates; in
115 contrast, other Cas nucleases non-specifically degrade only ssRNA (Cas13a)¹¹ or ssRNA and
116 ssDNA (Cas12g)²⁵ upon RNA targeting, or only ssDNA upon dsDNA targeting (Cas12a)¹⁴ (**Fig.**
117 **2b and Extended Data Fig. 9a**). Of the three collateral substrates, ssRNA and ssDNA were more
118 efficiently cleaved than ssDNA by Cas12a2 (**Fig. 2c and Extended Data Fig. 9b**). Also, similar

119 to Cas13a, complementary ssDNA and dsDNA do not activate any Cas12a2 non-specific
120 nuclease activity (**Extended Data Fig. 9a**), while dsRNA is not a substrate of collateral cleavage
121 (**Extended Data Fig. 9c**).

122
123 To examine if Cas12a2 activity is reliant on detecting a ‘non-self’ signal adjacent to the target
124 (called a protospacer flanking signal or PFS)¹¹, we performed *in vitro* cleavage assays in which
125 target RNA sequences were flanked on the 3’ side with a ‘self’ sequence complementary to the
126 crRNA repeat (5'-AUCUA-3’), the ‘non-self’ PFS used in our *in vivo* assay (5'-GAAAG-3’), or a
127 ‘flankless’ RNA complementary to the guide region of the crRNA, but containing no PFS (**Fig. 2b**).
128 Interestingly, only the RNA target containing the ‘non-self’ PFS activated collateral nuclease
129 activity, demonstrating that specific nucleotides on the 3’ end of the RNA target are essential for
130 activating the collateral activity of Cas12a2. Thus, Cas12a2 uses a “non-self activation”
131 mechanism distinct from RNA-targeting systems that rely on tag:anti-tag “self deactivation”
132 mechanisms^{11,26,27}. Additionally, introducing disruptive mutations to any of the three RuvC motifs
133 or conserved cysteines within the putative Zinc finger domain abolished all non-specific cleavage
134 (**Fig. 2d and Extended Data Fig. 9d**), consistent with our *in vivo* plasmid interference results
135 (**Fig. 1g**).

136
137 Our biochemical assays demonstrated Cas12a2 could quickly remove a FAM label from linear
138 dsDNA substrates, but it was unclear if Cas12a2 could degrade DNA lacking available 5’ or 3’
139 ends, such as supercoiled dsDNA. We therefore challenged crRNA-guided Cas12a2 with an RNA
140 target and a supercoiled pUC19 plasmid. Importantly, pUC19 does not contain any sequence
141 complementary to the Cas12a2 crRNA guide. We observed that, in the presence of target RNA,
142 SuCas12a2 rapidly nicked, linearized, and degraded pUC19 DNA, with the DNA fully degraded
143 within 60 minutes (**Fig. 2e**). This rapid destruction of supercoiled plasmid contrasts with the slow
144 and incomplete linearization of plasmid DNA by Cas12a nucleases²⁸. These data suggest a

145 mechanism where activated SuCas12a2 is able to robustly hydrolyze the phosphodiester
146 backbone of non-specific DNA whether it is supercoiled, nicked or linear. Comparison to Cas12a
147 (dsDNA targeting with collateral ssDNase), Cas13a (ssRNA targeting with collateral ssRNase),
148 and Cas13g (ssRNA targeting with collateral ssRNase and ssDNase) demonstrated that the RNA-
149 targeting ssRNase, ssDNase, and dsDNase are unique to SuCas12a2 (**Extended Data Fig. 9a**).
150 Collectively, these *in vitro* results reveal that crRNAs guide SuCas12a2 to RNA targets, activating
151 RuvC-dependent cleavage of ssRNA, ssDNA, and dsDNA, with these activities in part or in total
152 potentially underlying the Abi phenotype.

153

154 **Cas12a2 exhibits PFS and targeting flexibility while evading Cas12a anti-CRISPR proteins**
155 Although our *in vitro* data indicated an underlying mechanism for the Cas12a2 Abi phenotype, we
156 wanted to understand in greater depth the targeting limitations of these distinct enzymes. In
157 particular, we wanted to better understand the stringency of non-self PFS sequence recognition
158 and penalties for mismatches between the crRNA and target. We therefore challenged
159 SuCas12a2 with a library of plasmids encoding all possible 1,024 flanking sequences on the 3'
160 side of the RNA-target to the -5 position (**Extended Data Fig. 10a**). We found that SuCas12a2
161 depleted approximately half of all sequences in the library, suggesting a PFS recognition
162 mechanism more stringent than that of Cas13, but still more promiscuous than that of most DNA-
163 targeting systems (**Fig. 3a**). The depleted sequences were generally A-rich in line with a 5'-
164 GAAAG-3' PFS but could not be fully captured by a single consensus motif (**Fig. 3a and Extended**
165 **Data Fig. 10b-c**). We further validated individual depleted sequences, including representatives
166 within five unique motifs recognized by SuCas12a2 but not by Pb2Cas12a known among Cas12a
167 nucleases for flexible PAM recognition (**Fig. 3b and Extended Data Fig. 10**)²⁹. Consistent with
168 its function as an RNA-targeting nuclease, the recognized sequences were broad but did not
169 follow the expected profile if Cas12a2 is principally evaluating tag:anti-tag complementarity.
170 These results further supported a mechanism where PFS recognition by SuCas12a2 operates

171 similar to type III systems that require recognition of a PFS or rPAM (RNA PAM) to activate³⁰⁻³³
172 and distinct from the evaluation of tag:anti-tag complementarity used by RNA-targeting Cas13^{11,34}
173 and other type III CRISPR-Cas systems^{26,27}.

174
175 Most DNA and RNA-targeting Cas nucleases have shown high sensitivity to mismatches within a
176 seed region, where a single mismatch between the crRNA guide and target disrupts binding^{11,17,35-}
177³⁷. Therefore, to identify if SuCas12a2 relies on a seed region, we evaluated how SuCas12a2
178 tolerates mismatches in our cell-based assay (**Fig. 3c**). Interestingly, SuCas12a2 accommodated
179 single and double mismatches across the target, with PFS-distal mutations exerting more adverse
180 effects on plasmid targeting. To completely disrupt SuCas12a2 targeting, four mismatches were
181 needed throughout the guide (**Fig. 3c**) or up to 10 mismatches on the 3' end of a 24-nt guide
182 (**Extended Data Fig. 11**). The flexible PFS recognition and a tolerance for guide:target
183 mismatches indicates SuCas12a2 exhibits promiscuous target recognition and appears to lack a
184 canonical seed.

185
186 Collectively, the distinct activities of Cas12a2 compared to Cas12a suggested that tandem
187 systems possessing both nucleases may act cooperatively to broaden the effectiveness against
188 foreign viruses and plasmids. In particular, we hypothesized that the unique structural features of
189 Cas12a2 might prevent the escape of viruses encoding anti-CRISPR proteins that block Cas12a
190 function³⁸⁻⁴⁰. Consistent with this hypothesis, only one (AcrVA2.1) of seven Cas12a anti-CRISPRs
191 was able to impair Cas12a2 function, albeit only partially (**Fig. 3d and Extended Data Fig. 12a-**
192 **b**). Notably, AcrVA5 also exhibited no inhibitory activity despite SuCas12a2 possessing the
193 conserved lysine chemically modified by this Acr to block PAM recognition⁴¹ (**Fig. 3d and**
194 **Extended Data Fig. 12c**). The limited ability of Cas12a Acrs to inhibit SuCas12a2 further
195 underscores the distinct properties of these nucleases and the capacity of Cas12a and Cas12a2
196 to complement each other in nature.

197

198 **Triggered Cas12a2 enacts widespread DNA damage and impairs growth**

199 Although our initial results indicate Cas12a2 causes an Abi phenotype, it was unclear if the Abi
200 mechanism causes cell dormancy or cell death. Recently it was shown that, upon recognizing an
201 RNA target, Cas13a mediates widespread RNA degradation that drives cellular dormancy and
202 suppresses phage infection³. Introducing Cas13a from *Leptotrichia shahii* (LsCas13a) into our
203 modified plasmid interference assay, we observed that LsCas13a reduced plasmid transformation
204 similar to Cas12a2 in the absence of antibiotic selection for the target plasmid (**Extended Data**
205 **Fig. 13**). To verify that loss of the nuclease- and crRNA-encoding plasmids does not contribute
206 to this result, we evaluated growth of *E. coli* in liquid culture following induction of SuCas12a2,
207 LbCas12a, or LsCas13a with a targeting crRNA under different antibiotic selection conditions,
208 including a no-antibiotic condition. Under these conditions, both SuCas12a2 and LsCas13a
209 suppressed culture growth even when the target plasmids were not selected for, while LbCas12a
210 only suppressed growth in the presence of the target plasmid antibiotic (**Fig. 4a**).

211

212 Our comparison to LsCas13a suggested that the growth suppression by SuCas12a2 could occur
213 through non-specific RNA cleavage, causing cell dormancy, while our *in vitro* data indicated that
214 non-specific dsDNA cleavage could also suppress growth by causing cell death. To evaluate if
215 the cells containing SuCas12a2 were undergoing cell death, we performed a cell viability assay
216 with propidium iodide for both Cas12a2 and Cas13a. We observed only a small percentage
217 (~10%) of cell death in both Cas12a2 and Cas13a after 4 hours. Thus, although the indiscriminate
218 nuclease activities of Cas12a2 cause some cell death, the primary result of Cas12a2 activity is
219 better described as a cell dormancy phenotype (**Fig. 4b**).

220

221 Although Cas12a2 appears to cause dormancy, it was unclear which of the several indiscriminate
222 nuclease activities are involved. To determine if SuCas12a2 causes dormancy through RNA

223 cleavage, total cellular RNAs were examined under targeting and non-targeting conditions.
224 Compared to the bacteria expressing Cas13a, Cas12a2 yielded less RNA degradation, where
225 rRNAs appeared intact while RNAs the size of tRNAs were depleted (**Fig. 4c and Extended Data**
226 **Fig. 14**).

227
228 Given the less extensive RNA degradation under targeting conditions, we asked if the
229 indiscriminate dsDNase activity of SuCas12a2 was detectable in the context of the Abi phenotype.
230 We reasoned that widespread dsDNA damage caused by SuCas12a2 would trigger an SOS
231 response, impairing growth^{42,43}. In line with this assertion, plasmid targeting with SuCas12a2 but
232 neither LbCas12a nor LsCas13a significantly induced GFP expression from an SOS-responsive
233 reporter construct⁴⁴ compared to a non-target control (**Fig. 4d and Extended Data Fig. 15**).
234 Furthermore, SuCas12a2-targeting cultures diverged into two sub-populations in the absence of
235 antibiotic selection: one represented by compact cells with reduced DNA content and another
236 represented by filamentous cells with high DNA content (**Fig. 4e and Extended Data Fig. 16-17**).
237 Cultures expressing LbCas12a and LsCas13a did not exhibit noticeable differences in cell sizes
238 and DNA content for the target and non-target plasmids (**Fig. 4e and Extended Data Fig. 16-**
239 **17**). Previous studies with other CRISPR-Cas systems that specifically targeted the bacterial
240 chromosome observed similar morphological changes⁴⁵⁻⁴⁷, suggesting these distinct
241 morphologies are due to dsDNA damage. These results demonstrate that RNA targeting by
242 SuCas12a2 causes dsDNA damage of the bacterial chromosome that in turn induces the SOS
243 response and Abi in bacteria, reflecting a distinct mechanism of immunity that relies on
244 indiscriminate dsDNase activity. Consistent with this observation, recent cryo-EM structures
245 reveal Cas12a2 binds and cuts dsDNA with a mechanism completely distinct from all other
246 CRISPR associated nucleases, while structure-guided mutants with impaired *in vitro* collateral
247 dsDNase but not ssRNase and ssDNase activities abolished *in vivo* defense activity²⁰.

248

249 **Cas12a2 can be repurposed for programmable RNA detection**

250 CRISPR single-effector nucleases have been repurposed for a myriad of applications from gene
251 editing to molecular diagnostics. To determine if Cas12a2 could be repurposed as a
252 biotechnological tool, we programmed SuCas12a2 to detect RNA. We programmed apo-
253 SuCas12a2 with a crRNA guide complementary to an RNA target and incubated the complex with
254 a ssDNA or ssRNA beacon that fluoresces upon cleavage due to separation of a fluorophore and
255 a quencher (**Fig. 4f**). Using this approach, we were able to detect RNA using both ssDNA and
256 RNA probes at 37°C and room temperature, with a limit of detection within the range observed
257 for other single-subunit Cas nucleases¹⁸ (**Fig. 4f and Extended Data Fig. 18**). These data
258 indicate that SuCas12a2 can be readily repurposed as a tool for applications in science and
259 medicine. We anticipate that the unique activities of this enzyme can be further leveraged to
260 expand the CRISPR-based toolkit.

261

262 **Discussion**

263 Collectively, our data support a model in which Cas12a2 nucleases exhibit RNA-triggered
264 degradation of cytoplasmic dsDNA and to some extent RNA, impeding host cell growth and
265 eliciting an Abi phenotype (**Fig. 4h**). This mechanism contrasts with targeted invader clearance
266 or Abi activities exhibited by other CRISPR-Cas systems. Specifically, the mechanism exhibited
267 by Cas12a2 is reminiscent of the recently described CBASS defense system, which relies on the
268 indiscriminate double-stranded DNase NucC that degrades the host cell DNA and kills the cell¹².
269 Interestingly, some type III systems encode NucC enzymes, suggesting that other CRISPR-Cas
270 systems have convergently evolved to use a similar DNA degrading Abi mechanism^{13,48}.

271

272 In addition to damaging the genome and inducing the SOS response, SuCas12a2 exhibits
273 promiscuous RNA recognition through a flexible PFS and mismatch tolerance. This flexibility
274 could be particularly advantageous against rapidly evolving phages and could complement

275 precise recognition and clearance of DNA targets by Cas12a in organisms that encode both
276 Cas12a and Cas12a2 adjacent to a single CRISPR array (**Fig. 1 and Extended Data Figure 1**).
277 This dual-nuclease strategy would be akin to bacteria encoding multiple CRISPR-Cas systems
278 targeting the same invader⁴⁹. However, more work is needed to understand how these two
279 nucleases work together to counter infections.

280
281 The combination of nuclease-mediated crRNA biogenesis, RNA targeting, and collateral cleavage
282 of ssRNA, ssDNA, and in particular dsDNA sets Cas12a2 apart from other known Cas nucleases.
283 The apparent need to recognize the A-rich flanking sequence by SuCas12a2 to activate the
284 indiscriminate RuvC nuclease activity strongly indicates that Cas12a2 must bind a correct PFS
285 adjacent to the RNA target to activate cleavage rather than rely on complementarity between the
286 repeat tag and target anti-tag pair to distinguish self from non-self sequences typical of several
287 other RNA-targeting Cas nucleases and complexes^{11,26,27,50}. Investigating the underlying
288 molecular basis of target recognition and activation of collateral cleavage by Cas12a2 could
289 reveal new mechanisms employed by CRISPR nucleases for discriminating self from non-self
290 targets. Recent cryo-EM structures of Cas12a2 at stages of RNA-targeting and collateral dsDNA
291 capture are already fulfilling this need²⁰.

292
293 Cas12a2 holds substantial potential for CRISPR technologies. As a proof-of-principle
294 demonstration, we showed that SuCas12a2 can be repurposed for RNA detection with a limit of
295 detection comparable to existing single-effector based tools¹⁸. Beyond the ability to detect RNA,
296 we envision a variety of SuCas12a2 applications that expand and enhance the CRISPR-based
297 tool kit. RNA-triggered dsDNA cleavage could allow for programmable killing of prokaryotic and
298 eukaryotic cells with various applications, including programmable shaping of microbial
299 communities, cancer therapeutics, and counterselection to enhance genome editing. Additionally,
300 the ability of Cas12a2 and Cas12a to utilize the same crRNA sequence yet recognize distinct

301 nucleic acid species (RNA versus ssDNA and dsDNA) and elicit distinct non-specific cleavage
302 activities (ssRNA, ssDNA, and dsDNA (Cas12a2) versus ssDNA (Cas12a)) could augment
303 existing Cas12a applications by incorporating Cas12a2. By further exploring the properties of
304 SuCas12a2 and its homologs, we expect the advent of new and improved CRISPR technologies
305 that could broadly benefit society.

306

307 REFERENCES

- 308 1. Lopatina, A., Tal, N. & Sorek, R. Abortive Infection: Bacterial Suicide as an Antiviral Immune
309 Strategy. *Annu. Rev. Virol.* **7**, 371–384 (2020).
- 310 2. Koonin, E. V. & Krupovic, M. Origin of programmed cell death from antiviral defense? *Proc.*
311 *Natl. Acad. Sci.* **116**, 16167–16169 (2019).
- 312 3. Meeske, A. J., Nakandakari-Higa, S. & Marraffini, L. A. Cas13-induced cellular dormancy
313 prevents the rise of CRISPR-resistant bacteriophage. *Nature* **570**, 241–245 (2019).
- 314 4. Rostøl, J. T. & Marraffini, L. Non-specific degradation of transcripts promotes plasmid
315 clearance during type III-A CRISPR-Cas immunity. *Nat. Microbiol.* **4**, 656–662 (2019).
- 316 5. Rostøl, J. T. *et al.* The Card1 nuclease provides defence during type III CRISPR immunity.
317 *Nature* **590**, 624–629 (2021).
- 318 6. VanderWal, A. R., Park, J.-U., Polevoda, B., Kellogg, E. H. & O'Connell, M. R. CRISPR-
319 Csx28 forms a Cas13b-activated membrane pore required for robust CRISPR-Cas adaptive
320 immunity. 2021.11.02.466367 (2021) doi:10.1101/2021.11.02.466367.
- 321 7. Kazlauskiene, M., Kostiuk, G., Venclovas, Č., Tamulaitis, G. & Siksnys, V. A cyclic
322 oligonucleotide signaling pathway in type III CRISPR-Cas systems. *Science* **357**, 605–609
323 (2017).
- 324 8. Niewoehner, O. *et al.* Type III CRISPR–Cas systems produce cyclic oligoadenylate second
325 messengers. *Nature* **548**, 543–548 (2017).
- 326 9. Makarova, K. S., Anantharaman, V., Grishin, N. V., Koonin, E. V. & Aravind, L. CARF and

327 WYL domains: ligand-binding regulators of prokaryotic defense systems. *Front. Genet.* **5**,
328 (2014).

329 10. Gootenberg, J. S. *et al.* Nucleic acid detection with CRISPR-Cas13a/C2c2. *Science* **356**,
330 438–442 (2017).

331 11. Abudayyeh, O. O. *et al.* C2c2 is a single-component programmable RNA-guided RNA-
332 targeting CRISPR effector. *Science* **353**, aaf5573 (2016).

333 12. Lau, R. K. *et al.* Structure and Mechanism of a Cyclic Trinucleotide-Activated Bacterial
334 Endonuclease Mediating Bacteriophage Immunity. *Mol. Cell* **77**, 723-733.e6 (2020).

335 13. Grüschorw, S., Adamson, C. S. & White, M. F. Specificity and sensitivity of an RNA targeting
336 type III CRISPR complex coupled with a NucC endonuclease effector. *Nucleic Acids Res.*
337 **49**, 13122–13134 (2021).

338 14. Chen, J. S. *et al.* CRISPR-Cas12a target binding unleashes indiscriminate single-stranded
339 DNase activity. *Science* eaar6245 (2018) doi:10.1126/science.aar6245.

340 15. Marino, N. D., Pinilla-Redondo, R. & Bondy-Denomy, J. CRISPR-Cas12a targeting of
341 ssDNA plays no detectable role in immunity. 2022.03.10.483831 (2022)
342 doi:10.1101/2022.03.10.483831.

343 16. Zetsche, B. *et al.* Cpf1 Is a Single RNA-Guided Endonuclease of a Class 2 CRISPR-Cas
344 System. *Cell* **163**, 759–771 (2015).

345 17. Jinek, M. *et al.* A Programmable Dual-RNA–Guided DNA Endonuclease in Adaptive
346 Bacterial Immunity. *Science* **337**, 816–821 (2012).

347 18. Huyke, D. A. *et al.* Fundamental limits of amplification-free CRISPR-Cas12 and Cas13
348 diagnostics. <http://biorxiv.org/lookup/doi/10.1101/2022.01.31.478567> (2022)
349 doi:10.1101/2022.01.31.478567.

350 19. Makarova, K. S., Wolf, Y. I. & Koonin, E. V. Classification and Nomenclature of CRISPR-
351 Cas Systems: Where from Here? *CRISPR J.* **1**, 325–336 (2018).

352 20. Bravo, J. P. K. *et al.* Large-scale structural rearrangements unleash indiscriminate nuclease

353 activity by CRISPR-Cas12a2. *Be Submitted.*

354 21. Fonfara, I., Richter, H., Bratovič, M., Rhun, A. L. & Charpentier, E. The CRISPR-associated
355 DNA-cleaving enzyme Cpf1 also processes precursor CRISPR RNA. *Nature* **532**, 517–521
356 (2016).

357 22. Swarts, D. C., van der Oost, J. & Jinek, M. Structural Basis for Guide RNA Processing and
358 Seed-Dependent DNA Targeting by CRISPR-Cas12a. *Mol. Cell* **66**, 221-233.e4 (2017).

359 23. East-Seletsky, A. *et al.* Two Distinct RNase Activities of CRISPR-C2c2 Enable Guide RNA
360 Processing and RNA Detection. *Nature* **538**, 270–273 (2016).

361 24. Samai, P. *et al.* Co-transcriptional DNA and RNA Cleavage during Type III CRISPR-Cas
362 Immunity. *Cell* **161**, 1164–1174 (2015).

363 25. Yan, W. X. *et al.* Functionally diverse type V CRISPR-Cas systems. *Science* **363**, 88–91
364 (2019).

365 26. Marraffini, L. A. & Sontheimer, E. J. Self vs. non-self discrimination during CRISPR RNA-
366 directed immunity. *Nature* **463**, 568–571 (2010).

367 27. Estrella, M. A., Kuo, F.-T. & Bailey, S. RNA-activated DNA cleavage by the Type III-B
368 CRISPR–Cas effector complex. *Genes Dev.* **30**, 460–470 (2016).

369 28. Murugan, K., Seetharam, A. S., Severin, A. J. & Sashital, D. G. CRISPR-Cas12a has
370 widespread off-target and dsDNA-nicking effects. *J. Biol. Chem.* **295**, 5538–5553 (2020).

371 29. Marshall, R. *et al.* Rapid and Scalable Characterization of CRISPR Technologies Using an
372 *E. coli* Cell-Free Transcription-Translation System. *Mol. Cell* **69**, 146-157.e3 (2018).

373 30. Elmore, J. R. *et al.* Bipartite recognition of target RNAs activates DNA cleavage by the Type
374 III-B CRISPR–Cas system. *Genes Dev.* **30**, 447–459 (2016).

375 31. Kazlauskiene, M., Tamulaitis, G., Kostiuk, G., Venclovas, Č. & Siksnys, V. Spatiotemporal
376 Control of Type III-A CRISPR-Cas Immunity: Coupling DNA Degradation with the Target
377 RNA Recognition. *Mol. Cell* **62**, 295–306 (2016).

378 32. Liu, T. Y., Iavarone, A. T. & Doudna, J. A. RNA and DNA Targeting by a Reconstituted

379 Thermus thermophilus Type III-A CRISPR-Cas System. *PLOS ONE* **12**, e0170552 (2017).

380 33. Han, W. *et al.* A type III-B CRISPR-Cas effector complex mediating massive target DNA
381 destruction. *Nucleic Acids Res.* **45**, 1983–1993 (2017).

382 34. Wang, B. *et al.* Structural basis for self-cleavage prevention by tag:anti-tag pairing
383 complementarity in type VI Cas13 CRISPR systems. *Mol. Cell* **81**, 1100-1115.e5 (2021).

384 35. Wiedenheft, B. *et al.* RNA-guided complex from a bacterial immune system enhances target
385 recognition through seed sequence interactions. *Proc. Natl. Acad. Sci.* **108**, 10092–10097
386 (2011).

387 36. Semenova, E. *et al.* Interference by clustered regularly interspaced short palindromic repeat
388 (CRISPR) RNA is governed by a seed sequence. *Proc. Natl. Acad. Sci. U. S. A.* **108**,
389 10098–10103 (2011).

390 37. Liu, L. *et al.* Two Distant Catalytic Sites Are Responsible for C2c2 RNase Activities. *Cell*
391 **168**, 121-134.e12 (2017).

392 38. Watters, K. E., Fellmann, C., Bai, H. B., Ren, S. M. & Doudna, J. A. Systematic discovery of
393 natural CRISPR-Cas12a inhibitors. *Science* **362**, 236–239 (2018).

394 39. Knott, G. J. *et al.* Broad-spectrum enzymatic inhibition of CRISPR-Cas12a. *Nat. Struct. Mol.*
395 *Biol.* **26**, 315–321 (2019).

396 40. Marino, N. D. *et al.* Discovery of widespread type I and type V CRISPR-Cas inhibitors.
397 *Science* **362**, 240–242 (2018).

398 41. Dong, L. *et al.* An anti-CRISPR protein disables type V Cas12a by acetylation. *Nat. Struct.*
399 *Mol. Biol.* **26**, 308–314 (2019).

400 42. Little, J. W. & Mount, D. W. The SOS regulatory system of *Escherichia coli*. *Cell* **29**, 11–22
401 (1982).

402 43. Janion, C. Some aspects of the SOS response system--a critical survey. *Acta Biochim. Pol.*
403 **48**, 599–610 (2001).

404 44. Chen, Z., Lu, M., Zou, D. & Wang, H. An *E. coli* SOS-EGFP biosensor for fast and sensitive

405 detection of DNA damaging agents. *J. Environ. Sci.* **24**, 541–549 (2012).

406 45. Vercoe, R. B. *et al.* Cytotoxic Chromosomal Targeting by CRISPR/Cas Systems Can
407 Reshape Bacterial Genomes and Expel or Remodel Pathogenicity Islands. *PLOS Genet.* **9**,
408 e1003454 (2013).

409 46. Cui, L. & Bikard, D. Consequences of Cas9 cleavage in the chromosome of *Escherichia*
410 *coli*. *Nucleic Acids Res.* **44**, 4243–4251 (2016).

411 47. Caliando, B. J. & Voigt, C. A. Targeted DNA degradation using a CRISPR device stably
412 carried in the host genome. *Nat. Commun.* **6**, 6989 (2015).

413 48. Nemudraia, A. *et al.* Sequence-specific capture and concentration of viral RNA by type III
414 CRISPR system enhances diagnostic. *Res. Sq.* rs.3.rs-1466718 (2022)
415 doi:10.21203/rs.3.rs-1466718/v1.

416 49. Silas, S. *et al.* Type III CRISPR-Cas systems can provide redundancy to counteract viral
417 escape from type I systems. *eLife* **6**, e27601 (2017).

418 50. Liu, L. *et al.* The Molecular Architecture for RNA-Guided RNA Cleavage by Cas13a. *Cell*
419 **170**, 714-726.e10 (2017).

420 51. Sievers, F. *et al.* Fast, scalable generation of high-quality protein multiple sequence
421 alignments using Clustal Omega. *Mol. Syst. Biol.* **7**, 539 (2011).

422 52. Kozlov, A. M., Darriba, D., Flouri, T., Morel, B. & Stamatakis, A. RAxML-NG: a fast, scalable
423 and user-friendly tool for maximum likelihood phylogenetic inference. *Bioinform.* (2019)
424 doi:10.1093/bioinformatics/btz305.

425 53. Kelley, L. A., Mezulis, S., Yates, C. M., Wass, M. N. & Sternberg, M. J. E. The Phyre2 web
426 portal for protein modeling, prediction and analysis. *Nat. Protoc.* **10**, 845–858 (2015).

427 54. Söding, J., Biegert, A. & Lupas, A. N. The HHpred interactive server for protein homology
428 detection and structure prediction. *Nucleic Acids Res.* **33**, W244-248 (2005).

429 55. Guzman, L. M., Belin, D., Carson, M. J. & Beckwith, J. Tight regulation, modulation, and
430 high-level expression by vectors containing the arabinose PBAD promoter. *J. Bacteriol.* **177**,

431 4121–4130 (1995).

432 56. Studier, F. W. Protein production by auto-induction in high density shaking cultures. *Protein*
433 *Expr. Purif.* **41**, 207–234 (2005).

434 57. Lapinaite, A. *et al.* DNA capture by a CRISPR-Cas9–guided adenine base editor. *Science*
435 **369**, 566–571 (2020).

436 58. Harris, C. J., Molnar, A., Müller, S. Y. & Baulcombe, D. C. FDF-PAGE: a powerful technique
437 revealing previously undetected small RNAs sequestered by complementary transcripts.

438 *Nucleic Acids Res.* **43**, 7590–7599 (2015).

439 59. Li, Z., Zhang, H., Xiao, R., Han, R. & Chang, L. Cryo-EM structure of the RNA-guided
440 ribonuclease Cas12g. *Nat. Chem. Biol.* **17**, 387–393 (2021).

441 60. Bushnell, B., Rood, J. & Singer, E. BBMerge – Accurate paired shotgun read merging via
442 overlap. *PLOS ONE* **12**, e0185056 (2017).

443 61. Green, M. R., Sambrook, J. & Sambrook, J. *Molecular cloning: a laboratory manual*. (Cold
444 Spring Harbor Laboratory Press, 2012).

445 62. Leenay, R. T. *et al.* Identifying and Visualizing Functional PAM Diversity across CRISPR-
446 Cas Systems. *Mol. Cell* **62**, 137–147 (2016).

447 63. Wandera, K. G. *et al.* An enhanced assay to characterize anti-CRISPR proteins using a cell-
448 free transcription-translation system. *Methods San Diego Calif* **172**, 42–50 (2020).

449 64. Swarts, D. C. & Jinek, M. Mechanistic Insights into the cis- and trans-Acting DNase
450 Activities of Cas12a. *Mol. Cell* **73**, 589–600.e4 (2019).

451 65. Dong, D. *et al.* The crystal structure of Cpf1 in complex with CRISPR RNA. *Nature* **532**,
452 522–526 (2016).

453 66. Yamano, T. *et al.* Crystal Structure of Cpf1 in Complex with Guide RNA and Target DNA.
454 *Cell* **165**, 949–962 (2016).

455

456 **ACKNOWLEDGMENTS:**

457 We thank Kira Makarova for guidance naming Cas12a2, Leonhard Fläxl for assistance with TXTL,
458 Fani Ttofali for assistance with plasmid cloning and testing, April Pawluk and Ahsen Özcan for
459 critical feedback on the manuscript. Plasmids pET28a-mH6-Cas12g1 (Addgene plasmid #
460 120879) and pACYC-Cas12g1 (Addgene plasmid # 120880) were gifts from Arbor Biosciences.
461 Plasmid pC001 was a gift from Feng Zhang (Addgene plasmid # 79150).

462

463 **Funding:** This work was supported by an ERC Consolidator grant (865973 to C.L.B.), the DARPA
464 Safe Genes program (HR0011-17-2-0042 to C.L.B.), the National Institutes of Health
465 (R35GM138080 to R.N.J.), and the Netherlands Organization for Scientific Research (NWO)
466 through a Rubicon Grant (project 019.193EN.032 to I.M.). The views, opinions, and/or findings
467 expressed should not be interpreted as representing the official views or policies of the
468 Department of Defense or the U.S. Government.

469

470 **Author contributions:** Conceptualization: O.D., G.C.N., R.N.J., and C.L.B.; Methodology: O.D.,
471 G.D. V.M.C., J.M., H.D., T.H., and D.K. Investigation: bioinformatic discovery of Cas12a2
472 orthologs - B.N.G. and O.D.; first observation of bacterial Abi: G.C.N.; phylogenetic analysis -
473 O.D.; discovery of RNA targeting: O.D., D.K., R.N.J., and C.L.B.; experimentation in *E. coli* - O.D.,
474 G.C.N., V.M.C., E.V., I.M., and J.W.; in TXTL - K.W. and J.W.; *in vitro* - V.M.C., D.K., H.D, T.H.
475 and J.M.; Writing – Original Draft: O.D., V.M.C., R.N.J., and C.L.B.; Writing – Review and Editing:
476 All authors; Visualization: O.D., D.K., T.H., H.D., R.N.J., and C.L.B.; Supervision: M.B.B., R.N.J.,
477 and C.L.B.; Funding Acquisition: R.N.J. and C.L.B.

478

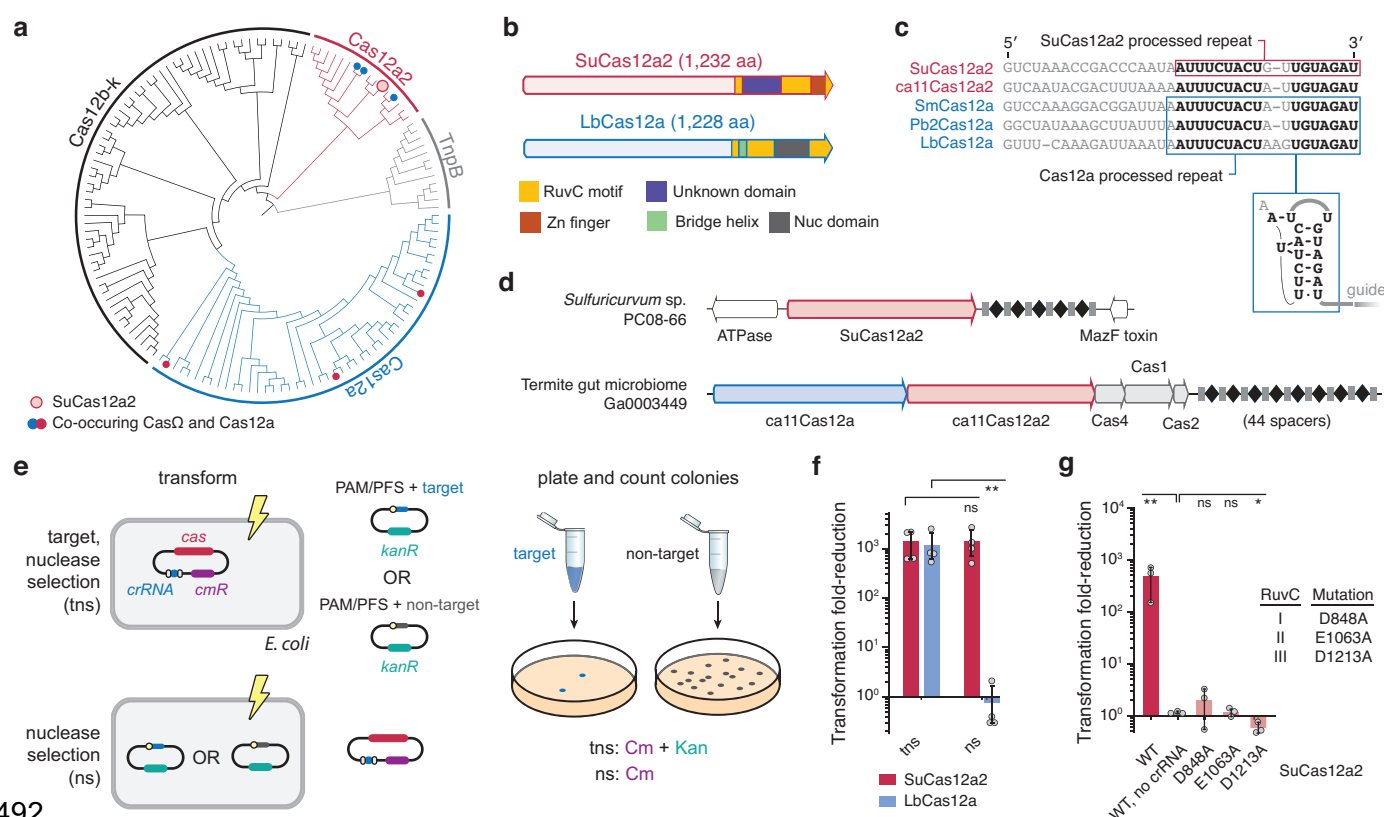
479 **Competing interests:** Benson Hill, O.D., R.N.J., and C.L.B. have filed provisional patent
480 applications on the related concepts. G.C.N., M.B.B., and B.N.G. are employees of Benson Hill.

481 C.L.B. is a co-founder of Locus Biosciences and is a scientific advisory board member of Benson
482 Hill. The other authors declare no competing financial interests.

483
484 **Data and materials availability:** The NGS data from the PAM depletion assay and crRNA
485 sequencing data were deposited to NCBI GEO under the accession GSE178536. All other data
486 in the main text or the supplementary materials are available upon reasonable request.

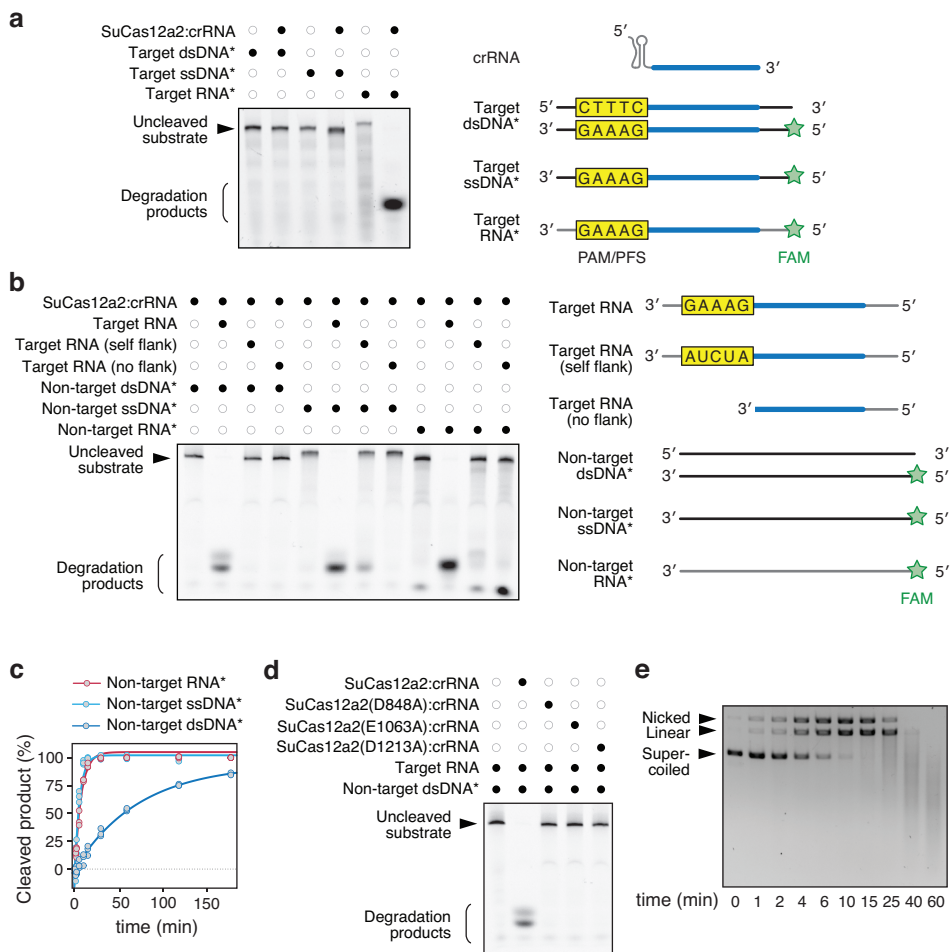
487
488 To review GEO accession GSE178536 prior to publication, go to
489 <https://www.ncbi.nlm.nih.gov/geo/query/acc.cgi?acc=GSE178536> and enter the token
490 mhuzayihxyfncf.

491 FIGURE LEGENDS



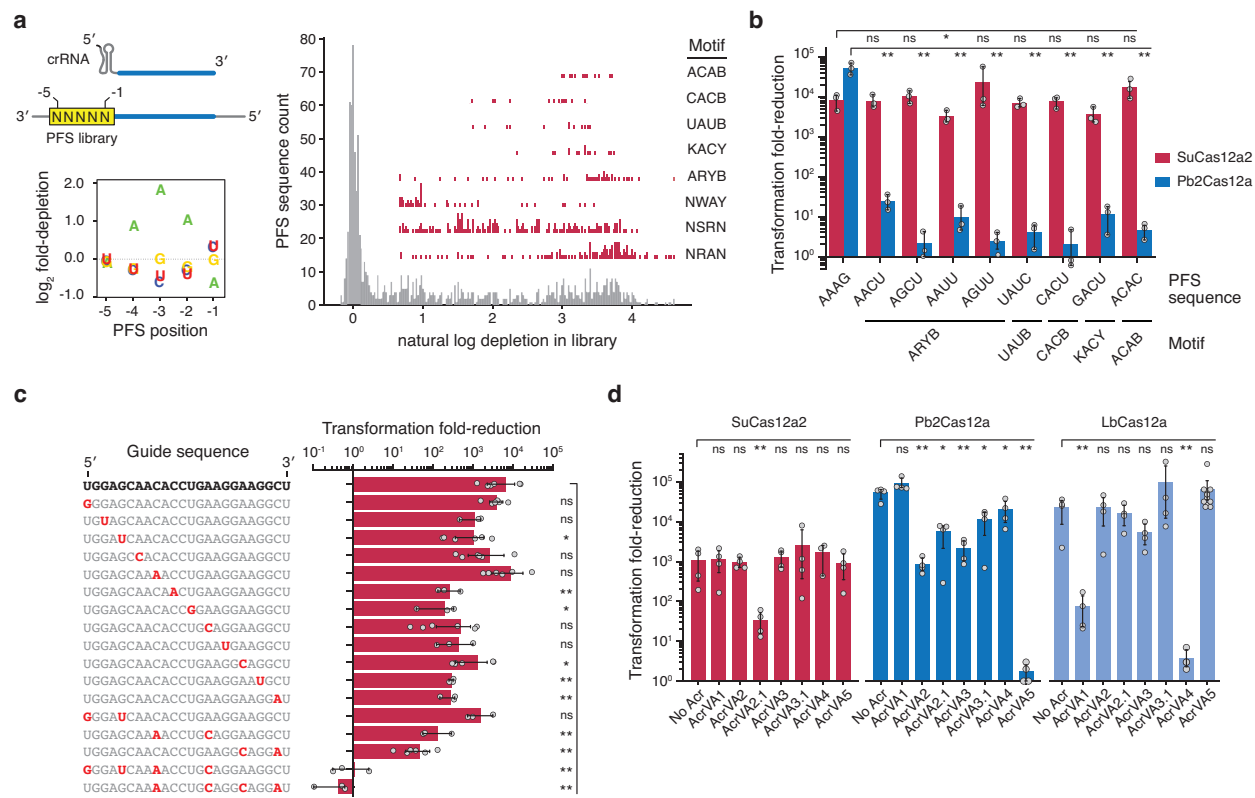
492

Fig. 1 | Cas12a2 nucleases form a distinct clade within type V Cas12 nucleases. **(a)** Maximum likelihood phylogenetic inference of selected Cas12 nucleases and identified Cas12a2 nucleases. See Extended Data Figure 1 for the detailed phylogeny. Systems with co-occurring Cas12a2 and Cas12a are indicated with filled red and blue circles. SuCas12a2 is indicated with an unfilled red circle. **(b)** Domain architecture of SuCas12a2 in comparison to LbCas12a. **(c)** Aligned direct repeats associated with representative Cas12a2 and Cas12a nucleases. Bolded nucleotides indicate conserved positions within the processed repeats for both nucleases. The predicted pseudoknot structure of the Cas12a repeat is diagrammed below. The loop of the hairpin (shown in gray) is variable. See Extended Data Figure 7 for pre-crRNA processing by SuCas12a2. **(d)** CRISPR system gene organizations within representative genomic loci encoding Cas12a2. Examples of systems encoding Cas12a2 as the sole Cas nuclease and also Cas12a are shown. **(e)** Diagram of the traditional (top - tns) and revised (bottom - ns) plasmid interference assay. **(f)** Reduction in plasmid transformation for SuCas12a2 and LbCas12a2 under target plasmid and nuclease plasmid selection. **(g)** Reduction in plasmid transformation of SuCas12a2 RuvC mutants under target and nuclease selection.



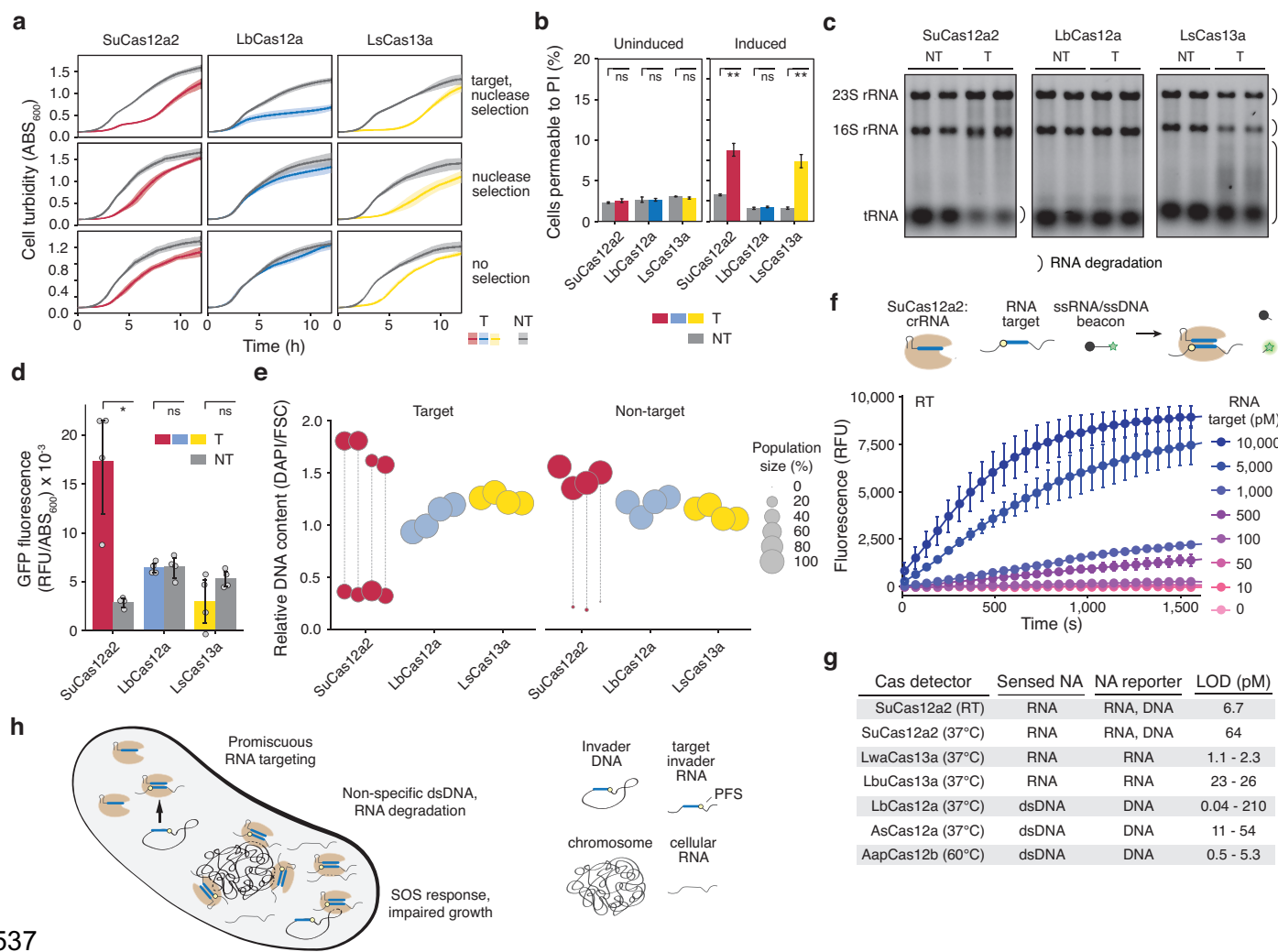
508

509 **Fig. 2 | RNA target recognition by SuCas12a2 triggers degradation of ssRNA, ssDNA and dsDNA**
510 *in vitro*. (a) Direct targeting of different FAM-labeled nucleic-acid substrates by a purified
511 SuCas12a2:crRNA complex, * indicates a FAM-labeled substrate, and diagrams to the right
512 indicate substrates. (b) Collateral cleavage of FAM-labeled non-target nucleic-acid substrates by
513 the SuCas12a2:crRNA complex with different target RNA substrates after 1 hour. Target RNA:
514 non-self flanking sequence on the 3' end. Self flank: flanking sequence mutated to the reverse
515 complement of the crRNA repeat tag. No flank: only the reverse complement of the crRNA guide.
516 Diagrams of target RNAs and non-target nucleic acids are diagrammed to the right. (c) Time
517 course of RNA-triggered collateral cleavage of labeled non-target RNA, ssDNA, or dsDNA. See
518 Extended Data Figure 9b for representative gel images. (d) Impact of mutating each of the three
519 RuvC motifs on RNA-triggered collateral cleavage of dsDNA. All results are representative of
520 three independent experiments. (e) Time course of RNA-triggered collateral cleavage of non-
521 target plasmid DNA. Plasmid DNA was visualized with ethidium bromide.



522

523 **Fig. 3 |** SuCas12a2 exhibits promiscuous targeting and resists anti-Cas12a proteins. **(a)**
524 Experimentally determined PFSs and motifs recognized by SuCas12a2 in *E. coli*. Motifs capture
525 position -4 through -1 of the PFS and are written 3' to 5'. B = C/G/U. K = G/U. R = G/A. W = A/U.
526 Y = C/U. Results are representative of two independent screens (see Extended Data Figure 10).
527 **(b)** Validation of selected PFSs identified in the screen and associated with SuCas12a2 but not
528 Pb2Cas12a. **(c)** Effect of guide mismatches on plasmid targeting by SuCas12a2 in *E. coli*. **(c)**
529 Effect of swapping direct repeats associated with SuCas12a2 and different Cas12a nucleases.
530 Error bars represent the mean and one standard deviation of at least three independent
531 experiments starting from separate colonies. ns: not significant. *: $p < 0.05$. **: $p < 0.005$. **(d)**
532 Extent of inhibition by known AcrVA proteins against SuCas12a2. Acrs were confirmed to exhibit
533 inhibitory activity against different Cas12a homologs in *E. coli* or in cell-free transcription-
534 translation reactions (see Extended Data Figure 12). Error bars represent the mean and one
535 standard deviation of at least three independent experiments starting from separate colonies. ns:
536 not significant. *: $p < 0.05$. **: $p < 0.005$.



537

538 **Fig. 4 |** SuCas12a2 causes abortive infection principally through collateral DNA degradation and
 539 can be harnessed for RNA detection. **(a)** Reduced transformation with targeting by SuCas12a2
 540 in the absence of target plasmid selection. The nuclease plasmid was transformed into cells with
 541 the target or non-target plasmid. **(b)** Percent of cells stained with propidium iodine indicative of
 542 loss of cell viability in the presence of a target or non-target plasmid. The Cas nuclease and
 543 associated crRNA were sampled prior to induction (uninduced) and after four hours (induced).
 544 Cells treated with isopropanol were used as a staining control. **(c)** Limited RNA degradation by
 545 SuCas12a2 compared to LsCas13a. Total RNA extracted from *E. coli* cells expressing the
 546 nuclease, crRNA, and target (T) or non-target (NT) construct 2 hours after nuclease and crRNA
 547 induction. Duplicate independent experiments are shown. See Extended Data Figure 14 for
 548 independent quadruplicates. **(d)** Expression from an SOS-responsive GFP reporter construct in
 549 *E. coli* following four hours of plasmid targeting by SuCas12a2, LbCas12a, or LsCas13a.
 550 Targeting was conducted without antibiotic selection. **(e)** Relative DNA content in *E. coli* following
 551 four hours of plasmid targeting by SuCas12a2, LbCas12a, or LsCas13a. Targeting was
 552 conducted without antibiotic selection. DAPI fluorescence and cell size were measured by flow
 553 cytometry analysis. Each circle or pair of vertically aligned circles represents major sub-
 554 populations from the same biological replicate. **(f)** Diagram of RNA detection assay. Limit of

555 detection for RNA detection for Cas12a2 incubated with a ssRNA beacon at room temperature
556 (RT). Error bars in a - h represent the mean and one standard deviation of at least three
557 independent experiments starting from separate colonies. ns: not significant. ns: not significant (p
558 ≥ 0.05). *: $p < 0.05$. **: $p < 0.005$ (g) Unamplified limit of detection (LOD) for several Cas
559 detectors¹⁸ compared to Cas12a2 determined by the velocity detection method. (h) Proposed
560 model for promiscuous RNA targeting and collateral DNA degradation by SuCas12a2 and its
561 outcome on cell growth.

562 **EXTENDED DATA**

563

564 **MATERIALS AND METHODS**

565

566 Identification of the putative Cas12a2 nucleases

567 Several Cas12a2 sequences were initially identified and tentatively classified as encoding Cas12a
568 nucleases¹⁶. These Cas12a2 protein sequences were used as seeds for BLASTP searches of
569 protein data in NCBI and for TBLASTN searches of metagenomic data in NCBI
570 (<https://www.ncbi.nlm.nih.gov>) and JGI (<https://img.jgi.doe.gov>) to identify additional putative
571 Cas12a2 nucleases.

572 Phylogenetic analysis of Cas12a2 proteins within type V systems

573 Amino acid sequences of Cas12a2 orthologs, Cas12a nucleases, representative nucleases from
574 all known type V subtypes, and TnpB orthologs were aligned using Clustal Omega⁵¹. The resulting
575 alignment was used to create a maximum likelihood phylogeny using RAxML-NG⁵² with the
576 following parameters: --model JTT+G --bs-metric fbp, tbe --tree pars{60}, rand{60} --seed 12345
577 --bs-trees autoMRE. TnpB sequences were used as an outgroup. The amino acid sequences
578 used in the creation of the phylogeny can be found in Extended Data File 1.

579 Domain annotation and structure prediction

580 Conserved motifs in SuCas12a2 were identified using MOTIF Search
581 (<https://www.genome.jp/tools/motif/>, accessed on 2021.06.15) and Phyre 2⁵³ (accessed on
582 2021.03.08). HHpred secondary structure predictions of Cas12a2 orthologous amino acid
583 sequences were performed to identify common secondary structure between Cas12a2 and
584 Cas12a that predicted the crRNA processing site of Cas12a2⁵⁴.

585 Strains and plasmids

586 All of the *in vivo* experiments, unless indicated otherwise, were performed in *E. coli* BL21(AI). For
587 propagation the cultures were grown in LB medium at 37°C with constant shaking at 225 - 250
588 rpm. *E. coli* strain TOP10 was used for plasmid cloning (**Extended Data Table 1, Tab 1**). All
589 primers, gBlocks, and oligos were obtained from Integrated DNA Technologies, unless specified
590 otherwise. Gibson assembly of plasmid construction was performed using NEBuilder HiFi DNA
591 Assembly Master Mix (New England Biolabs, E2621). Mutagenesis of the plasmids, including
592 small insertions and nucleotide substitutions, were done with Q5 Site-Directed Mutagenesis Kit
593 (New England Biolabs, E0554S). All of the nucleases together with crRNA, unless specified
594 otherwise, were expressed from plasmids containing p15A origin-of-replication and a
595 chloramphenicol resistance marker. The expression of the nucleases and crRNA was controlled
596 by a T7 promoter, unless specified otherwise. All target and non-target plasmids were created by
597 introducing protospacer sequences and corresponding flanking sequences into pBR322 or sc101
598 origin-of-replication plasmids bearing a kanamycin resistance cassette, unless specified
599 otherwise. Sequences encoding Cas12a2 orthologs (**Extended Data File 1**) were codon
600 optimized and synthesized by Genscript. Sequences encoding Pb2Cas12a from *Prevotella*
601 *bryantii* B14 (NCBI Accession: WP_039871282) LbCas12a from *Lachnospiraceae* bacterium
602 ND2006 (NCBI Accession: WP_035635841.1), FnCas12a from *Francisella tularensis* (NCBI
603 Accession: WP_104928540.1), AsCas12a from *Acidaminococcus* sp. BV3L6 (NCBI Accession:

604 WP_021736722.1), and Mb3Cas13a from *Moraxella bovoculi* (NCBI Accession:
605 WP_080946945.1)¹⁶ were codon optimized for expression in *E. coli* and ordered as gBlocks from
606 Integrated DNA Technologies. Sequences encoding anti-CRISPR proteins^{38,40} (**Extended Data**
607 **Table 1, Tab 3**) were codon-optimized for expression in *E. coli* and ordered as gBlocks from
608 Integrated DNA Technologies. The Acr genes were then PCR amplified and introduced into
609 pBAD24 plasmid backbone carrying ampicillin resistance cassette⁵⁵. The LsCas13a-encoding
610 plasmid pCBS2091 was ordered from Addgene (79150)¹¹. For detecting RecA-dependent SOS
611 response in *E. coli* BL21(AI), reporter plasmids pCBS2000, pCBS3611, and pCBS3616 were
612 created by introducing *recA* promoter, included 100 bp upstream of the predicted LexA binding
613 site, upstream of the GFP-encoding gene into plasmid pCBS198. Plasmids pCBS3611 and
614 pCBS3616 received an ampicillin resistance cassette from plasmid pCB672²⁹. The *recA* promoter
615 sequence was identified in the genome of *E. coli* BL21(AI) between positions 2,635,525 and
616 2,635,347 (NCBI Accession: CP047231.1). Control plasmids pCBS3616 and pCBS2002 without
617 the GFP-reporter genes were generated by PCR amplification of pCBS2000 and pCBS3616
618 followed by KLD assembly (New England Biolabs, M0554). The full list of plasmids used in the
619 study, including links to plasmid maps, can be found in **Extended Data Table 1, Tab 2**. Relevant
620 oligonucleotide, dsDNA, and RNA sequences are listed in **Extended Data Table 1, Tab 3**.

621 ***In vitro* characterization of SuCas12a2**

622 **Expression and purification of SuCas12a2**

623 N-terminal 6x His-tagged SuCas12a2 WT and mutant constructs were expressed in *E. coli*
624 Nico21(DE3) cells from a pACYC plasmid either lacking (apo) (plasmid 1416) or containing a
625 three-spacer CRISPR array (crRNA-guided) (plasmid 1408) using either an auto- or IPTG
626 induction. Autoinduction growths followed guidelines in Studier⁵⁶. Briefly, a solution containing
627 recommended concentrations of ZY media, MgSO₄, Metals Mix, 5052 and NPS autoinduction
628 buffers along with antibiotics needed for selection, was inoculated with bacteria from a glycerol
629 stock or a fresh transformation. The cells were grown for five hours at 37°C shaking at ~250 rpm
630 and then moved to 24°C where they were incubated for 24 h before harvesting via centrifugation
631 at 8K RPM for 25 min. Cell pellets were then stored at -80°C until purification. For the IPTG
632 induction, 1 L of TB media was inoculated with 20 ml of overnight growth and was grown at 37°C
633 until an OD₆₀₀ of 0.6. The cells were then cold-shocked on ice for 15 minutes and induced with
634 0.1 mM IPTG, followed by a 16-18 h incubation at 18°C. Cells were harvested by centrifugation.
635 Cells were lysed by sonication in Lysis buffer (25 mM Tris-pH 7.2, 500 mM NaCl, 10 mM
636 imidazole, 2 mM MgCl₂, 10% glycerol) in the presence of leupeptin, aprotinin, pepstatin, aepsf,
637 and lysozyme. The lysate was clarified by centrifugation at 36,400 x g for 35 minutes. Clarified
638 lysate was added to 5 ml of Ni-NTA resin and batch bound at 4°C for 30 minutes, and then washed
639 with 100 ml of lysis buffer. The protein was eluted with 50 ml of Ni-elution buffer (25mM Tris-pH
640 7.2, 500 mM NaCl, 250 mM imidazole, 2 MgCl₂, 10% glycerol). Fractions containing SuCas12a2
641 were desalting with a Hiprep 26/10 desalting column into low-salt buffer (25mM Tris-pCas12a22,
642 50 mM NaCl, 2 mM MgCl₂, 10% glycerol). SuCas12a2 + crRNA was then applied to a Hitrap Q
643 HP column anion exchange column while the apo SuCas12a2 was applied to a Hitrap SP HP
644 cation exchange column. The column was washed with 10% high-salt buffer (25mM Tris-pH 7.2,
645 1 M NaCl, 2 mM MgCl₂, 10% glycerol) followed by a gradient elution to 100 percent high salt

647 buffer 10 CV (50 ml). The fractions containing SuCas12a2 were concentrated using a 100 MWKO
648 concentrator to about 1 ml and then purified by size exclusion column chromatography over a
649 Hiload 26/600 superdex 200 pg column equilibrated in SEC buffer (100 mM HEPES-pH 7.2, 150
650 mM KCl, 2mM MgCl₂, 10% glycerol). The fractions containing SuCas12a2 were concentrated and
651 stored at -80°C.

652 Pre-crRNA processing

653 *Processing of a 3X pre-crRNA* - SuCas12a2 pre-CRISPRx3 RNA was in vitro transcribed using
654 the HiScribe™ T7 High Yield RNA Synthesis Kit (New England Biolabs). The template DNA was
655 derived from Jackson lab plasmid 1409 linearizing with the KpnI restriction enzyme. A
656 contaminating band that runs approximately at 130 nts was observed to be an artefact of the
657 reaction. Numerous strategies were attempted to prevent the transcription of this contaminating
658 band, to no success. In vitro transcribed RNA was cleaned on RNeasy spin columns (Qiagen).
659 1.5 μM of apo-SuCas12a2 was incubated with 1 mg of SuCas12a2 pre-CRISPRx3 RNA in 1X
660 3.1 Buffer from New England Biolabs (100 mM NaCl, 50 mM Tris-HCl, 10 mM MgCl₂, 100 mg/ml
661 BSA pH 7.9) and incubated at 25°C for various times. Samples were run on a gel (12%
662 polyacrylamide, 8M, TBE) alongside a ssRNA low range ladder (New England Biolabs) and
663 stained with SYBR gold (ThermoFisher Scientific).

664 *Processing a 1X crRNA with WT and crRNA processing mutants* - A synthetic crRNA with a 13
665 base 5' unprocessed overhang (**table S1 Tab 3**, smcrRNA) was refolded using the protocol
666 outlined in Lapinaite et al., 2020⁵⁷. In a 10 μl reaction, 150 nM of crRNA substrate was combined
667 with 1.5 μM WT, K784A, or K785A apo SuCas12a2 protein in NEB 3.1. The reactions were
668 incubated at 37°C for 1 h. The reactions were quenched with phenol and phenol:chloroform
669 extracted. The results were analyzed using 12% Urea-PAGE stained with SYBR-GOLD.

670 Nucleic acid cleavage assays

671 *Analysis of targeted cleavage* - 10 μl reactions of 250 nM SuCas12a2:crRNA with 100 nM of
672 complementary FAM-labeled synthetic oligonucleotide (i.e., ssDNA, dsDNA or RNA) in 1X NEB
673 3.1 buffer were incubated at 37°C for 1 h. Reactions were quenched with phenol and then
674 phenol:chloroform extracted. Results were analyzed using the FDF-PAGE method outlined in
675 Harris et al.,⁵⁸ and visualized for fluorescein fluorescence.

676 *Analysis of collateral cleavage* - 10 μl reactions of 250 nM SuCas12a2:crRNA, and 250 nM of
677 target (RNA complementary to the crRNA-guide) or non-target (RNA non-complementary to the
678 crRNA-guide) substrate and 100 nM of 5'-FAM labeled collateral substrate (ssDNA, dsDNA, RNA)
679 in 1X NEB 3.1 were incubated at 37°C for 1 h. Reactions were quenched with phenol and then
680 phenol:chloroform extracted. The results were analyzed using 12% Urea-PAGE and visualized
681 for fluorescein fluorescence.

682 *Analysis of flanking sequence requirements for activation* - 10 μl reactions of 250 nM
683 Cas12a2:crRNA, with 300 nM of different target ssRNAs: Self (flanked by sequence
684 complementary to the direct repeat of the crRNA), no flanks, and flanks containing a 5'-GAAA-3'
685 protospacer flanking sequence on the 3' side of the protospacer, and 100 nM of collateral 5'-FAM
686 dsDNA in 1X NEB 3.1 buffer were incubated at 37°C for 1 h. The reactions were quenched with
687 phenol and phenol:chloroform extracted. The results were analyzed using 12% Urea-PAGE and
688 visualized for fluorescein fluorescence.

689 *Kinetic analysis of collateral cleavage* - A single 100 μ l reaction containing 100 nM
690 Cas12a2:crRNA, 100 nM of target ssRNA (crRNA complementary) and 100 nM of different 5'-
691 FAM labeled collateral substrates (ssDNA, dsDNA, RNA) in 1X NEB 3.1 buffer was made. Time
692 points were taken at 1, 2, 5, 10, 15, 30, 60, 120, and 180 min by combining 10 μ l from the 100 μ l
693 reaction with phenol, followed by phenol:chloroform extraction. The results were analyzed using
694 12% Urea-PAGE and visualized for fluorescein fluorescence.

695 *Plasmid cleavage assay* - A 100 μ l reaction containing 14 nM Cas12a2:crRNA, 25 nM target RNA,
696 7 nM of pUC19 plasmid in 1X NEB 3.1 buffer was incubated at 37°C. At indicated time points, 10
697 μ l of the reaction was removed and quenched with phenol followed by phenol:chloroform
698 extraction. The reactions were visualized on 1% agarose with ethidium bromide.

699 Collateral cleavage comparison of Cas12a2 with Cas12a, Cas13a, and Cas12g
700 EnGen LbaCas12a (LbCas12a) was purchased from New England Biolabs (M0653S). 10- μ l
701 reactions containing 250 nM of LbCas12a and 500 nM of its cognate crRNA in 1X NEB 2.1 buffer
702 were incubated at 37°C with 200 nM of different target substrates (ssDNA, dsDNA, RNA) and 100
703 nM of different FAM labeled collateral substrates (ssDNA, dsDNA, RNA). After 1 h, the reactions
704 were quenched by phenol and phenol:chloroform extracted. The results were analyzed using 12%
705 Urea-PAGE and visualized for fluorescein fluorescence.

706 LwCas13a was purchased from MCLAB Molecular Cloning Laboratories (Cas13a-100). 10- μ l
707 reactions containing 250 nM of LwCas13a and 500 nM of its cognate crRNA in the provided 1X
708 Cas9 buffer (20 mM HEPES (pH 6.5), 5 mM MgCl₂, 100mM NaCl, 100 μ M EDTA) were incubated
709 at 37°C with 200 nM of different target substrates (ssDNA, dsDNA, RNA) and 100 nM of different
710 FAM labeled collateral substrates (ssDNA, dsDNA, RNA). After 1 h, the reactions were quenched
711 by phenol and phenol:chloroform extracted. The results were analyzed using 12% Urea-PAGE
712 and visualized for fluorescein fluorescence.

713 AbCas12g was expressed in *E. coli* NiCo 21 DE3 using pET28a-mH6-Cas12g1 (Addgene plasmid
714 #120879) and initially purified as described previously²⁵. The protein was then transferred to low
715 salt buffer (25 mM HEPES pH 7.8, 50 mM NH₄Cl, 2 mM MgCl₂, 7 mM BME, 5% glycerol) by buffer
716 exchange and loaded over heparin followed by elution with a linear NaCl gradient and gel filtration
717 as described previously⁵⁹. Purified protein was flash frozen and stored at -80°C. The Cas12g1
718 non-coding plasmid pACYC-Cas12g1 (Addgene plasmid #120880) was used as a template for
719 PCR amplification of the AbCas12g tracrRNA sequence with Cas12gtracrRNA F and R primers
720 (Table S1 tab 3) in 2x Taq Master Mix (New England Biolabs). The non-coding plasmid was
721 removed with DpnI by incubation at 37°C for 1 h in CutSmart buffer (New England Biolabs). DNA
722 components were cleaned after PCR and DpnI digest with E.Z.N.A. Cycle Pure Kit (OMEGA
723 BioTek). The Cas12g tracrRNA was transcribed with HighScribe T7 Quick High Yield RNA
724 synthesis kit and cleaned with Monarch RNA cleanup kit (New England Biolabs). 10- μ l reactions
725 containing 250 nM of Cas12g, 500 nM of the Cas12g crRNA, and 1 μ M of Cas12g tracrRNA in
726 1X NEB 3.1 buffer were incubated at 37°C or 50°C with 200 nM of different target substrates
727 (ssDNA, dsDNA, RNA) and 100 nM of different FAM labeled collateral substrates (ssDNA,
728 dsDNA, RNA). After 1 h, the reactions were quenched by phenol and phenol:chloroform extracted.
729 The results were analyzed using 12% Urea-PAGE and visualized for fluorescein fluorescence.

730 To analyze SuCas12a2 collateral activity, 10- μ l reactions containing 250 nM of Cas12a2:crRNA,
731 200 nM of different target substrates (ssDNA, dsDNA, ssRNA) and 100 nM of different FAM
732 labeled collateral substrates (ssDNA, dsDNA, RNA) in 1X NEB 3.1 buffer were incubated at 37°C

733 for 1 h. The reactions were quenched with phenol and phenol:chloroform extracted. The results
734 were analyzed using 12% Urea-PAGE and visualized for fluorescein.

735

736 **RNA detection by Cas12a2 with ssRNA and ssDNA reporter probes**

737 Cas12a2 (100nM) was complexed with crRNA (120nM) in NEB 3.1 buffer (50 mM Tris-HCl pH
738 7.9, 100 mM NaCl, 10 mM MgCl₂, 100 µg/ml BSA) before combining with RNase or DNase Alert
739 (200nM, IDT) and Target RNA to the indicated concentrations in a 384 well plate (Greiner Bio-
740 One, Ref#. 784077). A background control was prepared with nuclease free water instead of
741 Target RNA. Reactions were monitored for Reporter fluorescence (RNase Alert: Ex. 485-20/ Em.
742 528-20, DNase Alert: Ex. 500-20/Em. 560-20) over time at either ambient conditions (RT) or 37°C
743 using a Synergy H4 Hybrid multi-mode microplate reader (BioTek instruments inc.). The slope of
744 the linear region (between 5 and 30 min) was determined at each concentration of target RNA
745 using GraphPad PRISM. Standard error of the linear fit was used as a proxy for standard
746 deviation, and the limit of detection was calculated as 3 x Standard Error of the water background
747 as in (ref. ¹⁸). Limit of detection was estimated by determining where the plot of V₀ vs. [Target
748 RNA] crosses the detection threshold.

749

750 **Cas12a2 characterization in *E. coli***

751 **crRNA sequencing and analysis**

752 The SuCas12a2 expression plasmid pCBS3568 containing the nuclease- and the crRNA-
753 encoding sequences and the no-crRNA control pCBS3569 were transformed into *E. coli* BL21(AI)
754 and the transformants were plated on selection pates. The resulting colonies were picked and
755 used to inoculate 2 ml overnight liquid cultures. The next day, the overnight cultures were used
756 to inoculate 25 ml of LB containing chloramphenicol to an OD₆₀₀ of approximately 0.05. Once the
757 growing cultures reached the OD₆₀₀ of 0.25 after approximately 40 min, expression of the
758 nuclease and the crRNA were induced with 1 mM isopropyl β-D-1-thiogalactopyranoside (IPTG)
759 and 0.2% L-arabinose. The induced cultures were harvested in the stationary phase by
760 centrifugation at 14,000 rpm and 4°C for 2 min. Afterwards, the cell pellets were immediately
761 frozen in liquid N₂ and stored at -80°C until further processing.

762 Total RNA was purified from cell pellets using Direct-zol RNA Miniprep Plus (Zymo Research,
763 R2072) following manufacturer's instructions. DNA was removed using Turbo DNase (Life
764 Technologies, AM2238). Between the individual processing steps RNA was purified using RNA
765 Clean & Concentrator kit (Zymo Research, R1017). Ribosomal RNA was removed from the
766 samples using RiboMinus Transcriptome Isolation Kit, bacteria (ThermoFisher Scientific,
767 K155004). 3'-phosphoryl groups were removed from RNA using T4 polynucleotide kinase (New
768 England Biolabs, M0201S). cDNA synthesis and library preparation was performed with NEBNext
769 Multiplex Small RNA Library Prep Set for Illumina (New England Biolabs, E7330S). Size selection
770 for fragments between 200 bp and 700 bp was performed with Select-a-Size DNA Clean &
771 Concentrator kit (Zymo Research, D4080). Finally, DNA was purified using AMPure XP beads
772 (Beckman Coulter, A63882) and quantified with the Qubit dsDNA HS assay kit (ThermoFisher
773 Scientific, Q32851) on DeNovix DS-11 FX (DeNovix).

774 Library sequencing was performed at the Helmholtz Center for Infectious Research (HZI) GMAK
775 facility in Braunschweig, Germany, using the MiSeq 300 sequencing method (Illumina). The
776 resulting paired-end reads were quality controlled, trimmed, and merged using BBTools⁶⁰

777 (sourceforge.net/projects/bbmap/). Afterwards, the reads were mapped to the crRNA expression
778 site on the plus strand of pCBS273 using Bowtie2 (<http://bowtie-bio.sourceforge.net/bowtie2/>).
779 The associated raw and process sequencing data as well the data processing steps can be found
780 on NCBI GEO (Accession: GSE178531).

781 Plasmid clearance assay in *E. coli*

782 Standard plasmid clearance assay was performed in *E. coli* BL21(AI) containing nuclease- and
783 crRNA-expressing plasmids. Bacterial cultures were grown overnight and used to inoculate fresh
784 LB medium containing chloramphenicol to an OD₆₀₀ of 0.05 - 0.1. Subsequently, these cultures
785 were grown until the OD₆₀₀ reached approximately 0.25, at which time 1 mM IPTG and 0.2% L-
786 arabinose were added for induction. Once the cultures reached the OD₆₀₀ between 0.6 and 0.8,
787 the cells were harvested and made electrocompetent⁶¹. Electrocompetent cells were prepared
788 from four biological replicates. Immediately after, 1 μ l of 50 ng/ μ l of the target and non-target
789 plasmid were electroporated into 50 μ l of the electrocompetent *E. coli* cells. To achieve high
790 transformation efficiencies, the used plasmids were purified through ethanol precipitation and
791 quantified using the Qubit dsDNA HS Assay Kit (ThermoFisher Scientific, Q32851). The
792 electroporated cells were recovered for 1 hour at 37°C with shaking in 500 μ l LB containing 1 mM
793 IPTG and 0.2% L-arabinose without antibiotics. Afterwards, the cultures were sequentially diluted
794 to 10⁻⁵ in 10-fold increments. 5-10 μ l of each dilution were spotted on LB plates containing
795 antibiotics to select the nuclease-crRNA and the target/non-target plasmids. Additionally the
796 plates contained 0.3 mM IPTG and 0.2% L-arabinose. The plates were incubated overnight at
797 37°C.

798 The next day the colonies were manually counted and the resulting counts adjusted for the
799 dilution factor. Counts from the highest countable dilution were used to calculate transformation
800 fold reduction as a ratio between the colonies in the non-target condition divided by the colonies
801 in the target condition.

802 In a modification of the assay used to determine the cell suicide phenotype, the target and the
803 non-target plasmids were transformed into *E. coli* BL21(AI) first. Next, these cells were made
804 electrocompetent and the nuclease-crRNA plasmids were transformed in last.

805 When testing Acrs, the Acr plasmid (ampicillin) and the nuclease-crRNA plasmid
806 (chloramphenicol) were co-transformed, followed by electroporation of the target or non-target
807 plasmid (kanamycin).

808 Growth experiments

809 To investigate growth of the cultures under nuclease targeting conditions, the nuclease-crRNA
810 and the target/non-target plasmids were transformed into *E. coli* BL21(AI). The resulting
811 transformants were recovered in SOC medium and grown overnight with 0.2% glucose to inhibit
812 nuclease and crRNA expression. In the morning, the cells were harvested by centrifugation at
813 5,000 g for 2 min. The pellets were resuspended in LB and used to inoculate 200 μ l of LB medium
814 on a 96-well plate to the final OD₆₀₀ of 0.01. Depending on the experiment, the reactions contained
815 different combinations of antibiotics, IPTG, and L-arabinose. The plates were incubated in a
816 BioTek Synergy H1 plate reader at 37°C with vigorous shaking. The OD₆₀₀ of the cultures were
817 recorded every 3 min. Plasmid clearance assay was performed with the overnight cultures, as
818 described above.

819

820 PFS depletion assay in *E. coli*

821 To determine PFS preferences of SuCas12a2, a PFS depletion assay was performed. An oligo
822 library (ODpr23) consisting of 1,024 nucleotide combinations in place of a 5 nt PFS-encoding site
823 was synthesized by Integrated DNA Technologies. Using the ODpr23 oligo pool library in a
824 combination with primer ODpr24, targeting plasmid pCBS276 was PCR amplified using Q5
825 polymerase (New England Biolabs, M0543). The PCR products were gel-purified using
826 Zymoclean Gel DNA Recovery Kit (Zymo Research, D4007) and ligated using KLD reaction mix
827 (New England Biolabs, M0554). The ligated plasmids were purified using ethanol precipitation
828 and electroporated into *E. coli* TOP10. A total of 10 electroporation reactions were performed.
829 Following recovery of the electroporated cells in SOC medium, the individual reactions were
830 combined to inoculate 90 ml of LB medium containing kanamycin. 10 μ l from each electroporation
831 reaction were plated on selective LB medium to estimate the total number of transformed bacteria.
832 With the colony counts we estimated that the total number of transformed cells exceeded the
833 number of unique PAM sequences in the library (1,024) by approximately 2,300-fold. Plasmid
834 library DNA was purified from the combined overnight culture using ZymoPURE II Plasmid
835 Midiprep Kit (Zymo Research, D4201) and additionally cleaned by ethanol precipitation. Next, the
836 plasmid library was verified by Sanger sequencing.

837 The PAM plasmid library was transformed into electrocompetent *E. coli* BL21(AI) containing either
838 the SuCas12a2 nuclease-expressing plasmid pCBS273 and an empty plasmid control
839 pCBS3569. The electrocompetent cells were prepared as described above. Approximately 600
840 ng of the plasmid DNA were electroporated into 50 μ l volume of the competent cells. The
841 transformed bacteria were recovered in 500 μ l of SOC medium for 1 h at 37°C and were used to
842 inoculate 50 ml LB with 1 mM IPTG and 0.2% L-arabinose in the presence of kanamycin and
843 chloramphenicol. The cultures were grown for 13 hours before the cells were harvested by
844 centrifugation at 4,000 g for 15 min and the plasmid DNA extracted using ZymoPURE II Plasmid
845 Midiprep Kit (Zymo Research, D4201). Following recovery, bacteria were also plated on LB plates
846 containing kanamycin and chloramphenicol without the inducers. These plates were used to
847 estimate the total number of cells transformed with the plasmid library. The total number of
848 transformed cells estimated based on the colony counts exceeded the number of unique PAM
849 sequences in the library by approximately 1,700-fold for the cells containing the SuCas12a2-
850 crRNA plasmid (pCBS273) compared to 11,900-fold in the no-crRNA control (pCBS3569).

851 The region of the plasmid DNA which contained the target site including the PFS-encoding
852 sequence was PCR amplified using primers ODpr55 and ODpr56. The PCR reactions were
853 purified using AMPure XP beads (Beckman Coulter, A63882). The purified PCR products were
854 indexed using primers ODpr58, ODpr60, ODpr59, and ODpr61. The indexed PCR products were
855 purified using the AMPure XP beads, quantified with the Qubit assay (ThermoFisher Scientific,
856 Q32851), and sent for sequencing at the HZI GMAK facility in Braunschweig, Germany, using
857 MiSeq PE300 Illumina sequencing method.

858 Analysis of the PFS-encoding sequences depletion data as well as the creation of the PFS wheels
859 were performed as described previously⁶². PFS consensus motifs were defined manually. The
860 raw and the processed sequencing data as well as the data processing steps can be found on
861 NCBI GEO (Accession: GSE178530). Individual PFS sequences were validated using plasmid
862 clearance assay as described above.

863

864 Cell-free transcription-translation (TXTL) reactions

865 *In vitro assay to test Acr sensitivity of Cas12a nucleases* - Plasmids encoding Cas12a nuclease
866 were pre-expressed together with a plasmid encoding either a target or non-target crRNA in 9 μ l
867 of MyTXTL master mix (Arbor Biosciences) at the final concentration of 4 nM for each plasmid in
868 the total volume of 12 μ l. Acrs were pre-expressed separately, at the concentration of 4 nM in the
869 total volume of 12 μ l. Since the Acrs are encoded on linear DNA fragments, GamS at a final
870 concentration of 2 μ M, was added to prevent DNA degradation. All pre-expressions were carried
871 out at 29°C for 16 hours. The subsequent cleavage assay was performed by adding 1 μ l of each
872 pre-expression reaction to 9 μ l of fresh myTXTL mix. pCBS420 plasmid constitutively expressing
873 deGFP protein was used as a reporter at the final concentration of 1 nM. For quantification, four
874 3 μ l replicates per reaction were transferred onto a 96-well V-bottom plate (Corning Costar 3357).
875 The reactions were prepared using Echo 525 Liquid Handler (Beckman Coulter). Fluorescence
876 was measured on a BioTek Synergy H1 plate reader (Excitation: 485/20, Emission: 528/20).
877 Time-course measurements were run for 16 hours at 29°C, with 3 minute intervals between the
878 measurements.

879 All fold-repression values for plasmid reporter constructs represent the ratio of deGFP
880 concentrations after 16 h of reaction for the non-target over the target crRNA. For the experiments
881 measuring the inhibitory activity of Acrs, inhibition was calculated from endpoint expression values
882 after 16 h of expression according to the following formula⁶³.

883
$$\% \text{ Inhibition of nuclease activity} = 100 \times \frac{\text{GFPt-}, \text{AcrGF P nt-}, \text{Acr-GFPt-GF P nt-1}}{\text{GFPt-GFPnt-}}$$

884 The inhibition of nuclease activity [%] is defined by the ratio of fluorescence between GFP
885 targeting (GFPt-) and non-targeting (GFPnt-) Cas nucleases in the presence and absence of Acrs.
886 Quantification of SOS response

887 To measure the RecA-dependent SOS response, the nuclease-crRNA, the target/non-
888 target plasmids (pCBS276/pCBS3578, kanamycin), and the reporter *PrecA-gfp/no-gfp*
889 (pCBS3611/pCBS3616, ampicillin) plasmids were transformed into *E. coli* BL21(AI) sequentially.
890 Plasmids pCBS273 and pCBS3588 (chloramphenicol) were used to express SuCas12a2 and
891 LbCas12a nucleases, respectively. When measuring the RecA-dependent SOS-response in the
892 presence of LsCas13a, the nuclease expression plasmid pCBS361 (chloramphenicol) was used.
893 The target/non-target plasmids pCBS2004/pCBS612 (ampicillin) and *PrecA-gfp/no-gfp* plasmids
894 pCBS2000/pCBS2002 (kanamycin) were used. First, the cells were grown LB medium with 0.2%
895 glucose to inhibit expression of the nucleases and the crRNA. The bacteria were harvested from
896 the overnight cultures (15 ml) by centrifugation at 5,000 g for 2 minutes and resuspended in fresh
897 LB. Next, 200 μ l of fresh LB medium were inoculated on 96 well plates with the resuspended
898 bacteria from the overnight cultures. These cultures were grown in the presence of either
899 chloramphenicol, kanamycin, and ampicillin, chloramphenicol and ampicillin, or no antibiotics. For
900 induction of nuclease and crRNA expression 1 mM of IPTG and 0.2% L-arabinose were added.
901

902 The cultures were grown at 37°C with vigorous shaking. OD₆₀₀ and fluorescence
903 measurements (Excitation: 485/20, Emission: 528/20) were collected every 5 minutes on a BioTek
904 Synergy H1 plate reader. Four biological replicates were measured per experimental condition.
905 To determine if a change in fluorescence occurred as a result of nuclease targeting, first the
906 background fluorescence collected for the cultures with the *PrecA-no-gfp* plasmid

907 (pCBS3616/pCBS2002) was subtracted from the values obtained for the cultures with the GFP-
908 expressing plasmids for each time point (pCBS3611/pCBS2000). Next, the fluorescence values
909 were divided by the OD₆₀₀ values from the corresponding target and the non-target cultures.
910 Statistical significance was determined using Welch's t-test with unequal variance.

911 In parallel we performed a plasmid clearance assay with the washed overnight cultures
912 (**Extended Data Figure 15b**), as described above. For the lowest plated dilution cultures at the
913 OD₆₀₀ of ~0.1 were used.

914

915 Flow cytometry

916 For the flow cytometry measurements, *E. coli* BL21(AI) cells were sequentially
917 electroporated with the nuclease-encoding and target/non-target plasmids. The SuCas12a2- and
918 LbCas12a-expressing plasmids pCBS273 and pCBS3588 were used, respectively. Target
919 plasmid pCBS273 and non-target plasmid pCBS3578 were used. For the experiments involving
920 LsCas13a, nuclease-expression plasmid pCBS361 was used in combination with the target
921 plasmid pCBS2004 and non-target plasmid pCBS612. Following plasmid transformation, the *E.*
922 *coli* bacteria were recovered in SOC medium and grown overnight in LB with chloramphenicol,
923 kanamycin, and 0.2% glucose. Next, the cells were harvested at 5,000 g for 2 minutes and
924 resuspended in fresh LB. The resuspended bacteria were used to inoculate 15 ml cultures to the
925 OD₆₀₀ of ~0.01. These cultures were grown at 37°C with 220 rpm shaking for 6 hours without
926 antibiotics with 1 mM IPTG and 0.2% L-arabinose. Every 2 hours the OD₆₀₀ of the cultures was
927 measured and 500 µl samples were collected and centrifuged for 3 minutes at 5,000 g. The cell
928 pellets were then resuspended in 1x PBS containing 2 µg/ml 4',6-diamidino-2-phenylindole (DAPI,
929 ThermoFisher Scientific, 62248). The resuspended cells were stained for 10 minutes in the dark,
930 after which 10 µl were transferred into 240 µl of 1x PBS on a 96 well plate. DAPI fluorescence
931 was measured with Cytoflow Novocyte Quanteon flow cytometer as emission in the Pacific Blue
932 spectrum (455 nm). Data regarding the forward scatter (FSC) and the side scatter (SSC) were
933 also collected.

934 The resulting data were analyzed in Python. First, clusters of bacteria which exhibit distinct
935 FSC and Pacific Blue signals were identified using density-based spatial clustering of applications
936 with noise (DBSCAN <https://scikit-learn.org/stable/modules/generated/sklearn.cluster.DBSCAN.html>). Next, the ratios of the Pacific Blue to the FSC signal for each data
937 point and the percentage of the data points within each cluster were parsed from the clustering
938 data. The resulting values were plotted in the form of balloon plots. 60,000 events per sample
939 were analyzed.

941

942 Dead/Live staining

943 Dead and viable bacteria were estimated with the LIVE/DEAD BacLight™ Bacterial
944 Viability and Counting Kit (Molecular Probes, L34856). The measurements were performed with
945 Cytoflow Novocyte Quanteon flow cytometer. *E. coli* BL21(AI) bacteria were transformed with
946 nuclease, crRNA, and either target or non-target expression plasmids. For expressing
947 SuCas12a2 and LbCas12a with a target guide, plasmids pCBS273 and pCBS3588 were used,
948 respectively. Target expression plasmid pCBS2004 and non-target expression plasmid pCBS612
949 were used. For expressing LsCas13a with a target and non-target guides, plasmids pCBS273
950 and pCBS3578 were used, respectively. Cultures containing combinations of nuclease-guide and

951 target plasmids were grown for approximately 16 hours with 0.2% glucose inhibitor in four
952 biological replicates. Afterwards, 1 ml of each culture was harvested at 5,000 g for 3 minutes. The
953 resulting pellet was resuspended in 1 ml of fresh LB medium. 60 μ l of this suspension were used
954 to inoculate 20 ml of LB. There cultures were grown for 2 hours at 37°C with constant shaking at
955 220 rpm. The expression of the nucleases and the guides was induced with 0.2% arabinose and
956 0.01 mM IPTG. After 4 hours, OD600 of the cultures was measured. Volume of the cultures
957 corresponding to the OD600 1.0 was collected and processed as described in the kit manual.
958 Briefly, samples of the bacterial culture were spun in a centrifuge at 10,000 \times g for 3 minutes to
959 pellet the cells. The supernatant was removed and the pellet resuspended in 1 ml of 0.85% NaCl.
960 As a control for the dead cells, spectate pellet was first resuspended in 300 μ l 0.85% NaCl and
961 then 700 μ l 70% isopropyl alcohol (dead-cell suspension). The samples were incubated at room
962 temperature for 60 minutes, with mixing every 15 minutes. Next, the samples were centrifuged at
963 10,000 \times g for 3 minutes and washed in 1 ml 0.85% NaCl, followed by another centrifugation.
964 Finally, the samples were resuspended min 0.5 ml of 0.85% NaCl. 1 ml of master mix for staining
965 the cells contained 977 μ l of 0.85% NaCl, 1.5 μ l of Component A (3.34 mM SYTO 9 nucleic acid
966 stain), 1.5 μ l of Component B (30 mM propidium iodide(PI)), 10 μ l of Component C (beads), and
967 10 μ l of a sample. These reactions were incubated for 15 minutes at room temperature protected
968 from light. Fluorescence was collected in the green (e.g., fluorescein for SYTO 9) and red (Texas
969 Red for PI) channels. The dead cells in each sample were gated based on the dead-cell
970 suspension control treated with isopropyl alcohol. The percentage of dead cells stained with PI
971 was calculated from the total number of events without the beads. 50,000 events were counted
972 per sample.
973

974 *In vivo* RNA degradation

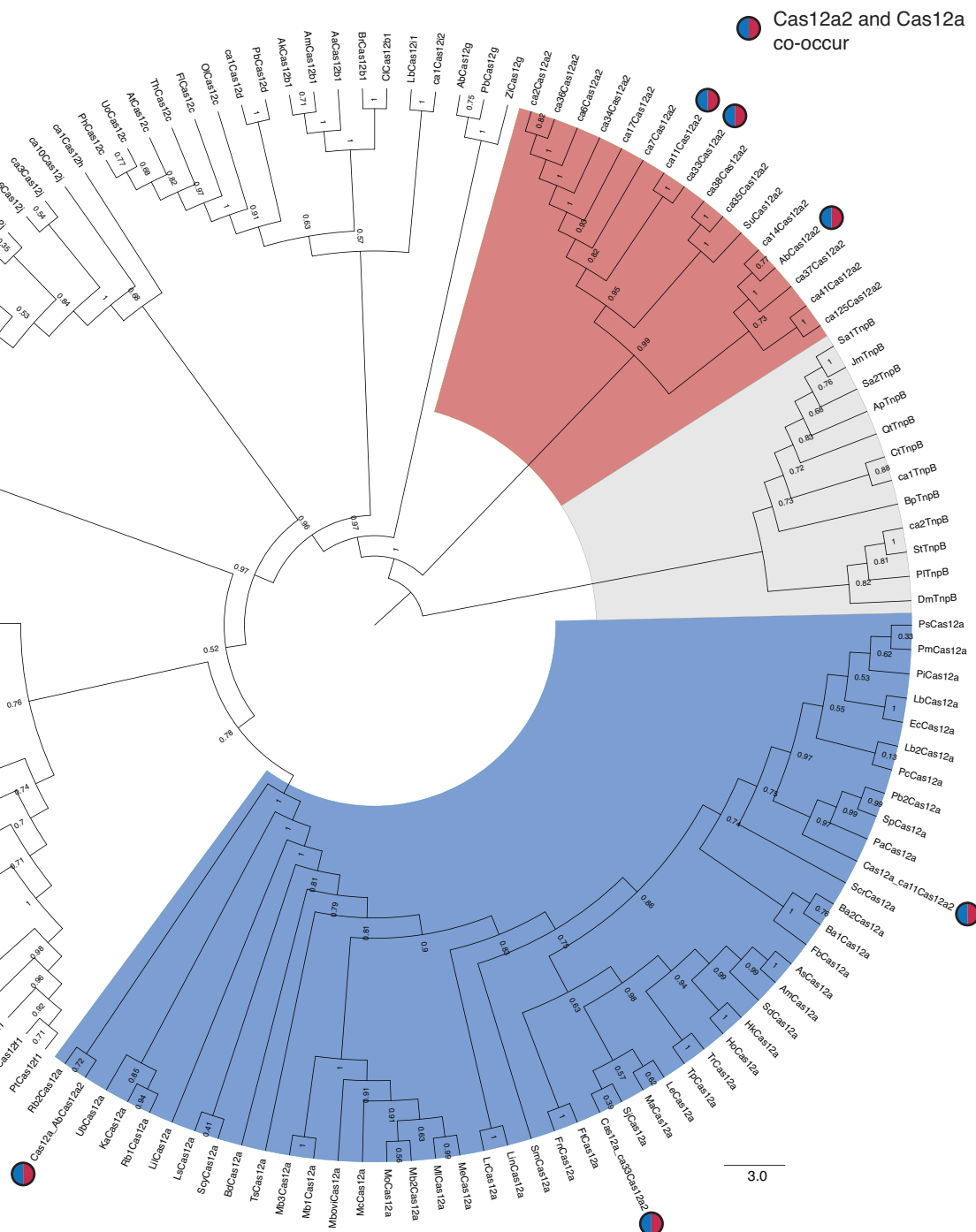
975 Samples corresponding to 1 ml of culture at OD600 0.4 of grown for dead/live staining, as
976 described above, were collected and centrifuged at 10,000 \times g for 3 minutes. The resulting pellets
977 were frozen in liquid nitrogen and stored -80°C until further processing. Total RNA was expected
978 using 1.5 ml of trizol and 1.5 ml of ethanol with Direct-zol RNA Miniprep kit (R2051, Zymo),
979 according to the manufacturer's instructions. The RNA was further purified with the RNA Clean &
980 Concentrator-5 kit (R1013, Zymo). 0.5 μ g of RNA from each sample in 5 μ l were combined with
981 2.5 μ l of RNA loading dye, heated to 70°C for 10 minutes, and subsequently chilled on ice for 2
982 minutes. The used RNA High-Range ladder was also heat-treated. The denatured samples (5 μ l)
983 and the leader (3 μ l) were loaded on a 1% TBE gel. The gel was run for 40 minutes at 120V.
984 Afterwards, the gel was stained for 30 min in ethidium bromide, washed for 10 ml, and imaged.
985

986 Microscopy

987 For confocal microscopy, the cells were grown as for the flow cytometry above. In 2 hour
988 intervals, 500 μ l of each culture were collected and centrifuged at 5,000 g for 3 minutes. Next, the
989 bacteria were diluted to approximately the same cell density and stained with 2 μ g/ml of FM4-64
990 dye (ThermoFisher Scientific, T13320) and 1 μ g/ml of DAPI (ThermoFisher Scientific, 62248).
991 Imaging was done on a Leica DMi6000B TCS-SP5 II Inverted Confocal Microscope at 1,000x
992 magnification.
993
994

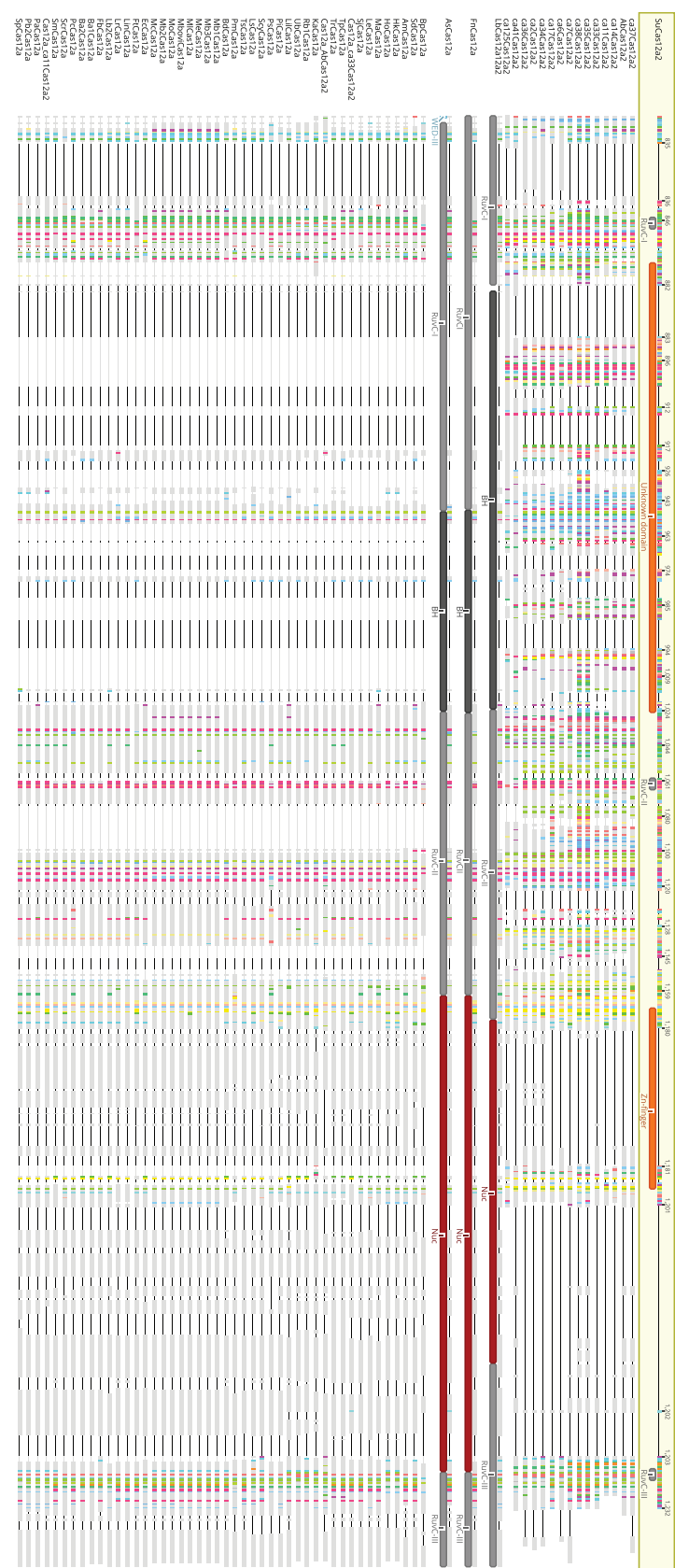
995 **EXTENDED DATA FIGURES**

996

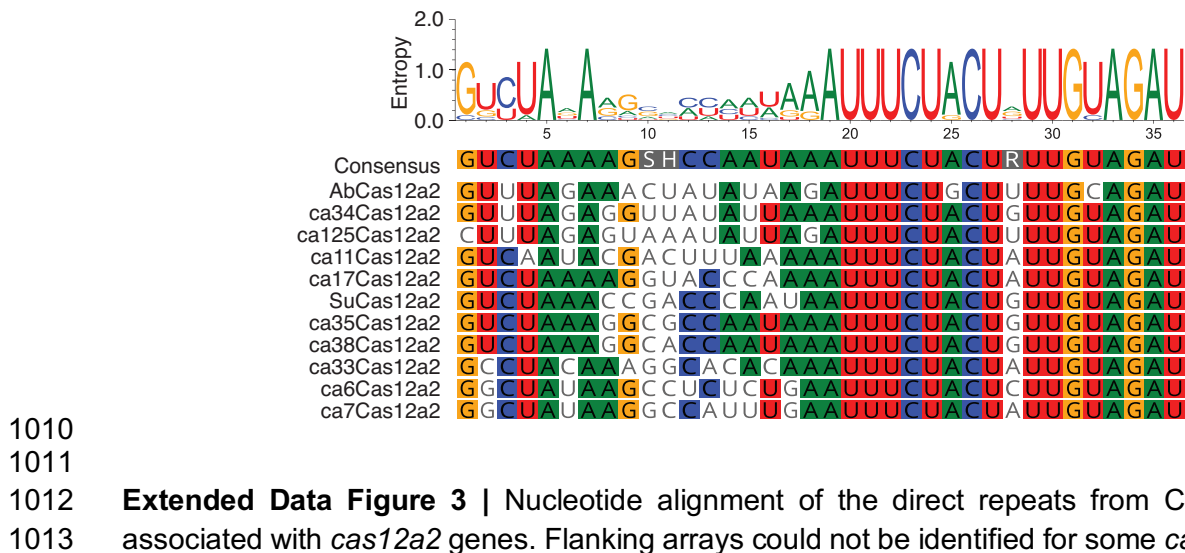


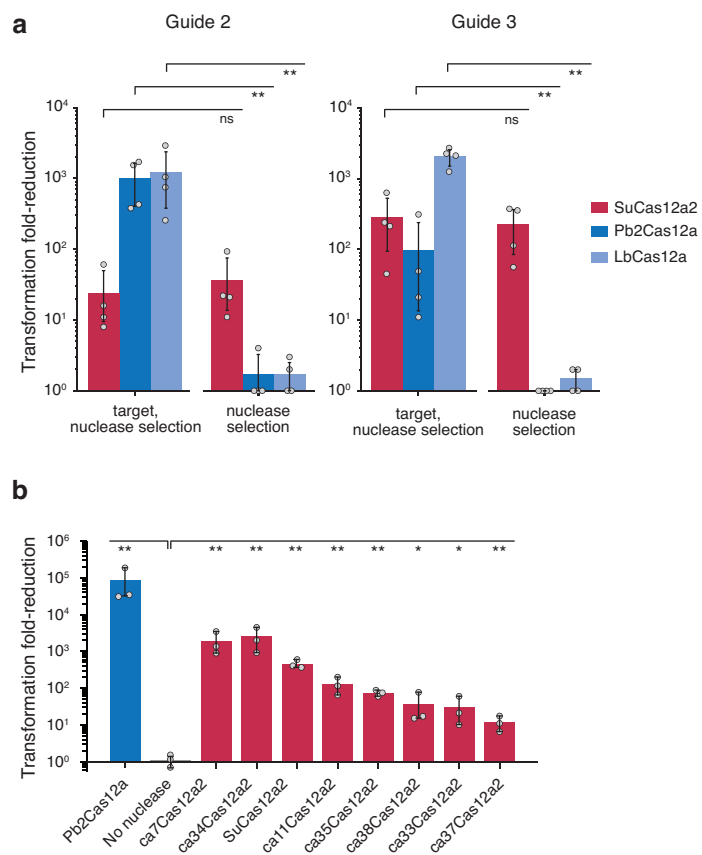
997

998 **Extended Data Figure 1 |** Maximum-likelihood phylogenetic inference of Cas12a2 and several
 999 other type V nucleases. The phylogenetic tree generated using amino acid sequences is an
 1000 enlarged and annotated version of Figure 1a. The shaded regions designate Cas12a2 (red),
 1001 Cas12a (blue), and TnpB (gray) orthologs. The blue and red filled circles indicate systems that
 1002 contain both Cas12a2 and Cas12a.



1005 **Extended Data Figure 2 |** Fragment of an amino-acid sequence alignment containing the RuvC
1006 domain within Cas12a2 and Cas12a orthologs. The domains in FnCas12a⁶⁴, LbCas12a⁶⁵, and
1007 AsCas12a⁶⁶ are based on crystal structures. The domains in SuCas12a2 were predicted using
1008 MOTIF search. The highlighted residues represent SuCas12a2 amino acids conserved in other
1009 Cas12a2 and Cas12a sequences. Numbering is shown in relation to SuCas12a2.

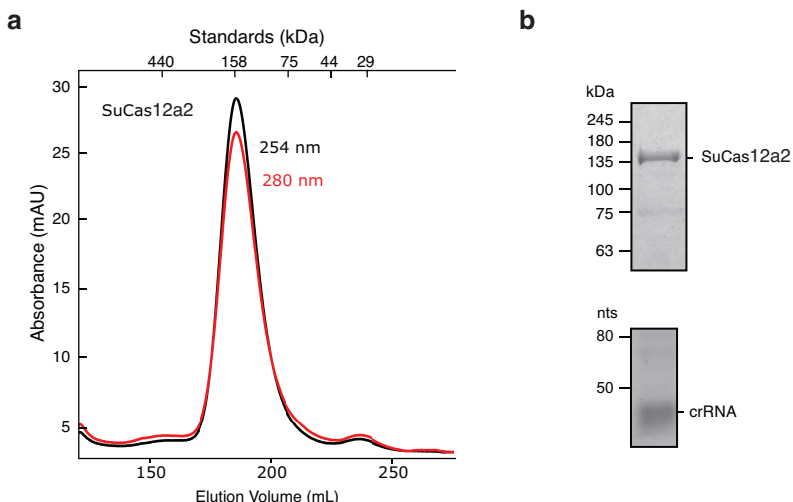




1014

1015 **Extended Data Figure 4 | Transformation reduction by SuCas12a2 and other Cas12a2 orthologs,**
1016 **LbCas12a, and Pb2Cas12a in *E. coli* BL21(AI). (a)** Different guide:target pairs tested under
1017 antibiotic selection of the nuclease and target plasmids or only the nuclease plasmid. **(b)** Different
1018 Cas12a2 orthologs tested under antibiotic selection of the nuclease and target plasmids. Error
1019 bars depict one standard deviation from the mean. Significance was calculated using Welch's t-
1020 test (* - p < 0.05, ** - p < 0.005).

1021



1022

1023 **Extended Data Figure 5 |** Purification of SuCas12a2. **(a)** Size exclusion chromatogram of purified
1024 SuCas12a2 bound to a co-expressed 3X crRNA guide over a Superdex 200 pg 26/600 column.
1025 Absorbance was measured at 254 nm and 280 nm. Molecular weight standards are indicated
1026 (top). **(b)** SDS-PAGE of purified SuCas12a2 + crRNA (top). Urea-PAGE gel of RNA acid-phenol-
1027 chloroform extracted from purified SuCas12a2 + crRNA (bottom).

crRNA Processing Loop

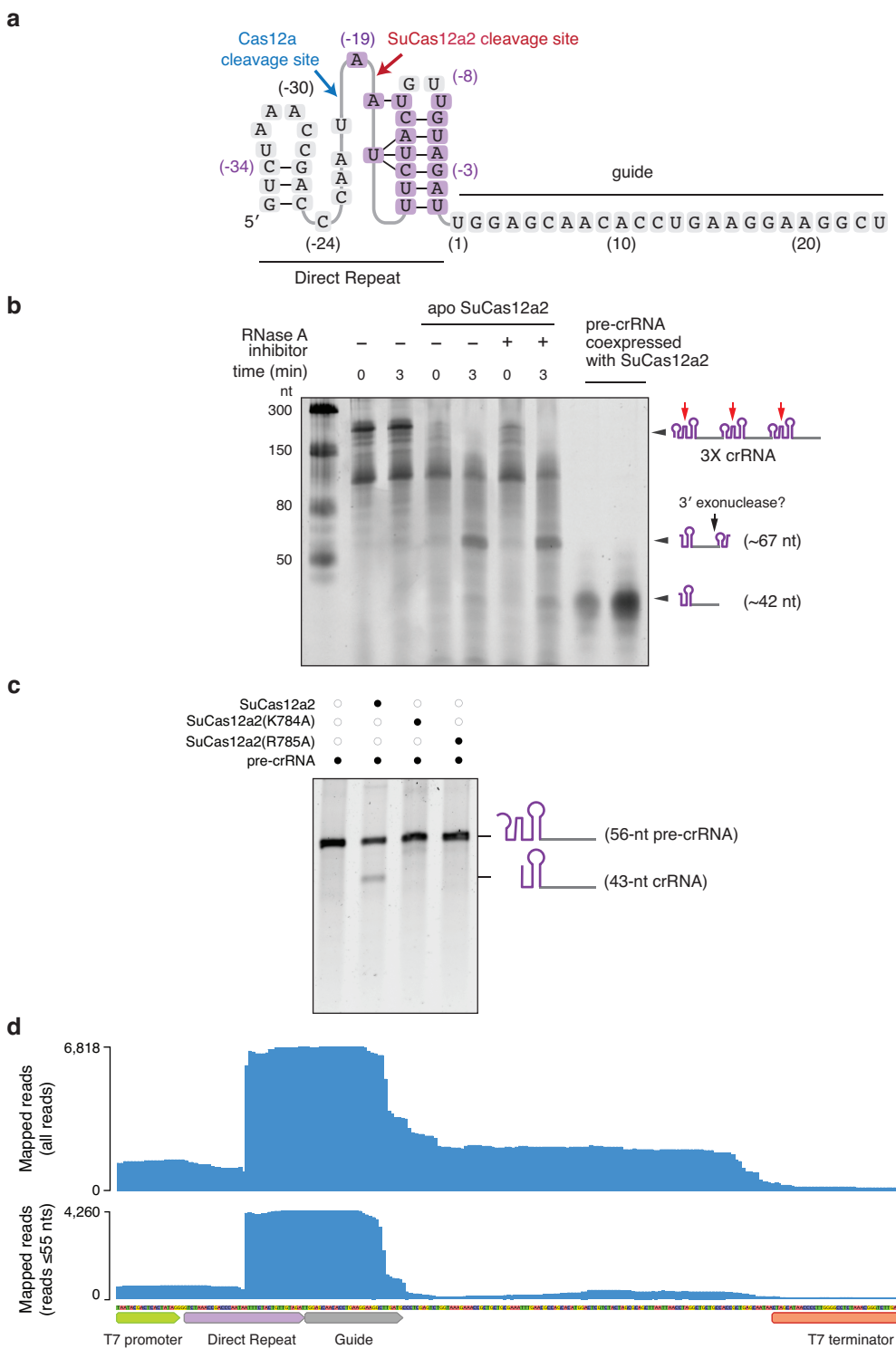
SuCas12a2WP_041148111.1	-----KRYGRLQFVCAFNAHIVPQN-17-DVQKRNVTEFNKKVNHAL---SDKEYVVIGIDRGL	851
LnCas12aWP_044910712.1	KVKVLESERVKWSKFYDEQFAVIFSVKNAD----CLDTTKDLNAEVMEQYSE-----SNRLLILRNT	886
BrCas12aWP_013282991.1	AIKKANEDIIIRNRRYTEDKFFLSSLSTYKNAD----ISARTLDYINDKVEEDTQD---SRMAVIVTRNL	892
ParbacCas12aKKR91555.1	-DGNKEKEVIQRRFAKDALTLLKIRLNFG----KHV-NLFDFNKLVNTELFA---KVPVKILGMDRGE	895
EuCAGCas12aWP_022501477.1	GHRKSKDIDIVKDKRYTEDKYFLYLPITINYK----IED---ENVNSKIIYEYIAK---QDNMNVIGIDRGE	893
EuCas12aWP_012739647.1	EVRTAQKDIVKDKRYTVDKYFIHTPITINYK----VTA---RNNVNDMVVKYIAQ---NDIIVIGIDRGE	883
MetCas12aWP_015504779.1	KTKKADHDIVDKRRTVDKMMFHVPIAMNFK----AIS---KPNLNKKVIDGID---DQDLKIIGIDRGE	851
CanCas12aAIZ56868.1	RYFKAHYDITKDRRYLNDKIYFHVPLTLNFK----ANG---KKNLNKVMVIEKFLS---DEKAHIIGIDRGE	862
HcCas12aWP_005398606.1	KYKEARFDIICKDRRYSEQFFFHVPIFNWD----IKT---NKNVNQIVQGMIKD---GEIKHIIIGIDRGE	920
AcCas12aWP_021736722.1	ITKEVSHIIKDRRTSDKFFFHVPIITNYQ----AAN-SPSKFNQRVNAYLKE---HPETPIIGIDRGE	911
SuccCas12aWP_031492824.1	IKKEATHDITKDKRFTSDKFFFHCPLTINYK----EGD---TKQFNNEVLSFLRG---NPDINIIGIDRGE	937
MiCas12aKKQ38174.1	----GNKVIDHCKRYSENKIFHVPLTLNRT----KNDSY---RFNAQINNF---LANNKDINIIGVDRGE	894
PcCas12aKKT48220.1	----GDRAYKRYTEKKIMFHMSLVLNTG----KGEIKQVQFNKIINQRISSSDNEMRVNVIGIDRGE	926
AnCas12aWP_027407524.1	KESVFNVDLIDLKRYTERKFYFHCPITLNFR----ADK---PIKYNEKINRFVEN---NPDVCIIIGIDRGE	843
ProteoCas12aWP_028830240.1	LKDKFDYDPIIKDKRYSQDKFFFHVPMVINYK----SEKLNLSKSLNNRNTENLQG----FTHIIIGIDRGE	784
PdCas12aWP_004356401.1	KVSLFTYDIYKMRYYMENKFLFHLSIVQNYK----AAN-DSAQLNSSATEYIRK---ADDLHIIIGIDRGE	946
LnNCCas12aWP_027109509.1	KESIFSVDIVKDKRYSQDKFFFHVPMVINYK----EQN---VSRFNDYIREILKK---SKNIRVIGIDRGE	815
BufbCas12aWP_027216152.1	PTRRLDYDIVKDKRYSQDKFMIHTSIIMNFG----AEE---NVSFDIVNVGVRN---EDKVNVIGIDRGE	837
OriCas12aWP_049895985.1	KTSTFDYDIDVKKDRRYCQDKFMLHLPITVNFG----TNE---SGKFNELVNNAIRA---DKDVNVIGIDRGE	834
PseudoCas12aWP_028248456.1	PTSKFGYDIIKDKRYSQDKFMLHLPITMNFG----VDE---TRRFNDVNDALRN---DEKVRVIGIDRGE	817
LnmaCas12aWP_044919442.1	ETSTFSYDIVKDKRYSQDKFTLHPIITMNFG----VDE---VKRFNDAVNSAIRI---DENVNVIGIDRGE	818
FnCas12a_3WP_004339290.1	KESVFEYDLIKDKRFTEDKFFFHCPITMNFK----SSG---ANKFNDIEINLLKE---KANDVHILSIDRGE	927
PmCas12aWP_018359861.1	ETSLFNQYDLVKKDKRFTEDKFFFHVPISTYK----NKK---ITNVNQMVDRYIAQ---NDDLQIIIGIDRGE	863
MxCas12aKDN25524.1	-KRQFVYDIIKDKRYSQDKFMLHLPITMNFG----VQGMTIKEFNKVNQSIQ---YDEVNVIGIDRGE	989
LpCas12aWP_020988726.1	LFEKLKYPILKDKRYSQDKFQFLHLPISLNFK----SKE---RLNFNLKVNEFLKR---NKDINIIGIDRGE	876
SmCas12aWP_037385181.1	ATSTFNYDIVKDKRYSQDKFQFLHLPITMNFK----AEG---IFNMNQRVNQFLKA---NPDINIIGIDRGE	866
FbCas12aCCB70584.1	NEKNKTIDIIKDKRFTVDKFQFHVPITMNFK----ATG---GSYINQTVLEYLQN---NPEVKIIGLDRGE	932
FlavbCas12aWP_045971446.1	AKNTFAYDLIKDKRYSQDKFQFHVPITMNFK----ATG---NSYINQDVLAYLKD---NPEVNIIGLDRGE	888
LnMCCas12aWP_044910713.1	EVSVFPYDIIKDKRYSQDKFQFHVPILMNFK----ADE---KKRINDDVIAIRS---NKGIIHIGIDRGE	842
LnNDCas12aWP_035635841.1	KTTTLSYDVYDKDKRFSEDQYELHIPIAINKC----PKN---IFKINTEVRLVLLKH---DDNPYVIGIDRGE	835
LnCoeCas12aWP_016301126.1	KESMFYDIDIIKDKRFTCDKYQFHVPIITMNFK----ALG---ENHFNRKVNRLIHD---AENMIIIGIDRGE	845
PorpCas12aWP_023936172.1	EESLFSEYDLVKDKRYSQDKFQFHVPITMNFK----CSA---GSKVNDMVNAHIRE---AKDMHIGIDRGE	883
PrevbCas12aWP_044110123.1	KQSNFSEYDLIKDKRYSQDKFQFHVPITLNFK----GMG---NGDINQMVREYIKT---TDDLHIIIGIDRGE	877
BoCas12aWP_009217842.1	KESKFYDIDIIKDKRYSQDKFQFHVPITMNFK----SVG---GSNINQLVKRHIRS---ATDLHIIIGIDRGE	868
PvCas12aWP_024988992.1	HTSTFKYDIIKDKRYSQDKFQFHVPITLNFK----ATG---QNNINPIVQEVIRO---NGITHIIGIDRGE	865
PbB_Cas12aEF170750.1	KESIFDYDILVKDKRYSQDKFQFHVPITMNFK----STG---NTNINQQVIDYLRT---EDDTHIIGIDRGE	869

**

Positively Charged Active Site Residues

1028

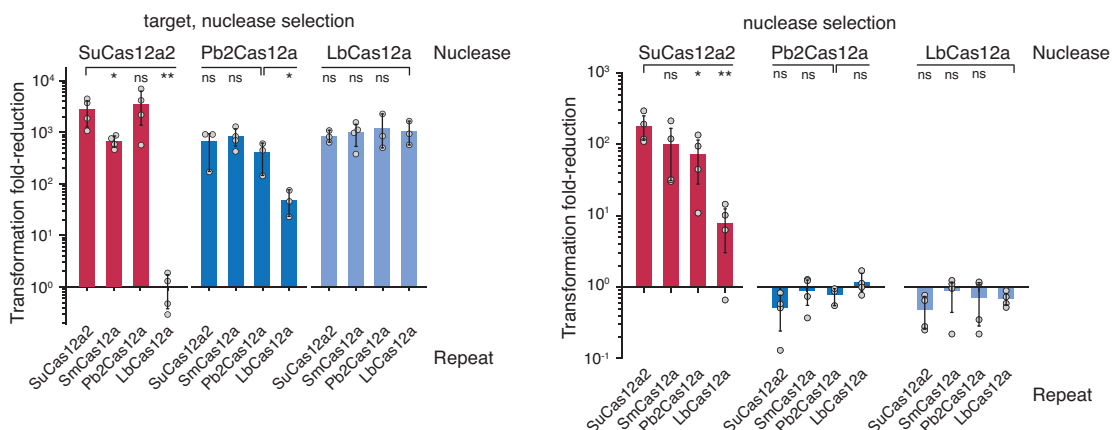
1029 **Extended Data Figure 6 |** Clustal Omega amino acid sequence alignment of SuCas12a2 with
1030 Cas12a sequences. Cas12a amino acids located within the loop involved in crRNA-processing
1031 are indicated in red. Conserved positively charged residues involved in processing²¹ are indicated.
1032 Although the putative crRNA-processing loop of Cas12a2 is not as long the positively charged
1033 residues appear to be conserved.



1034

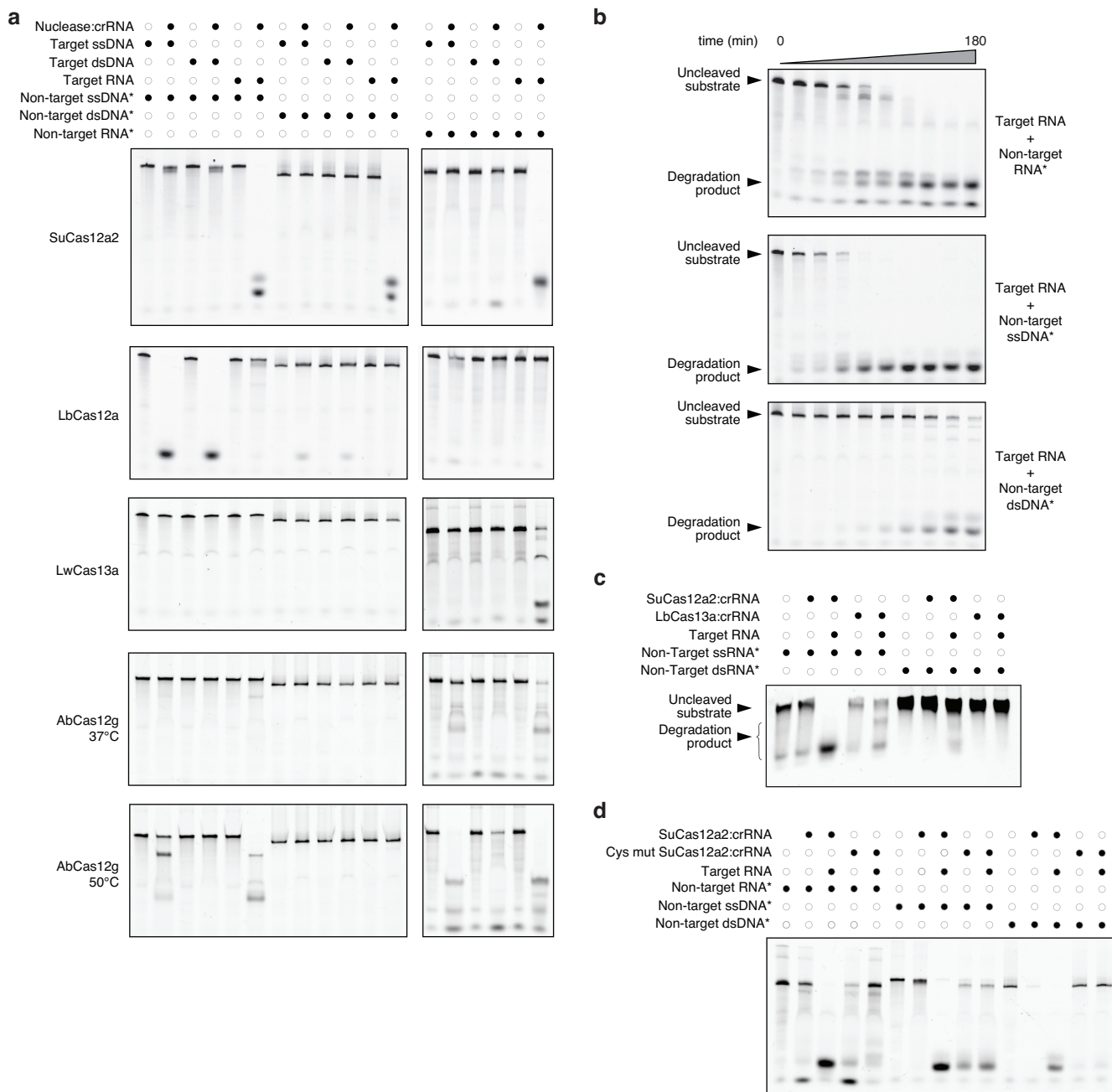
1035 **Extended Data Figure 7** | Pre-crRNA processing by SuCas12a2. **(a)** A diagram of the predicted
1036 secondary structure of the SuCas12a2 direct repeat. Cleavage sites of SuCas12a2 and Cas12a
1037 are indicated. **(b)** *In vitro* SuCas12a2-mediated cleavage of a pre-crRNA containing three direct
1038 repeats and three spacers (3X crRNA). Reactions containing apo-SuCas12a2 are indicated. Time
1039 points after mixing the cleavage reaction with apo-SuCas12a2 are indicated. The estimated sizes

1040 of the pre-crRNA and crRNAs after cleavage are indicated on the left. The last two lanes contain
1041 RNA extracted from SuCas12a2 co-expressed with a CRISPR array. The difference in size
1042 between the major crRNA band in the *in vitro* assay (~ 67 nt) and the crRNA extracted from
1043 SuCas12a2 bound to *E. coli*-expressed crRNA (~42) may be due to further trimming by 3'
1044 exonucleases in the cell. (c) *In vitro* processing of a 56-nt pre-crRNA incubated for 60 minutes in
1045 the presence of apo-Cas12a2 or two mutants predicted to disrupt crRNA processing. (d)
1046 Sequencing coverage of the cDNA mapped to the crRNA locus in *E. coli* BL21(AI) expressing
1047 SuCas12a2. Coverage for all of the quality-filtered reads above 10 nts as well as reads between
1048 10 and 55 nts mapped to the plus strand are shown.



1049

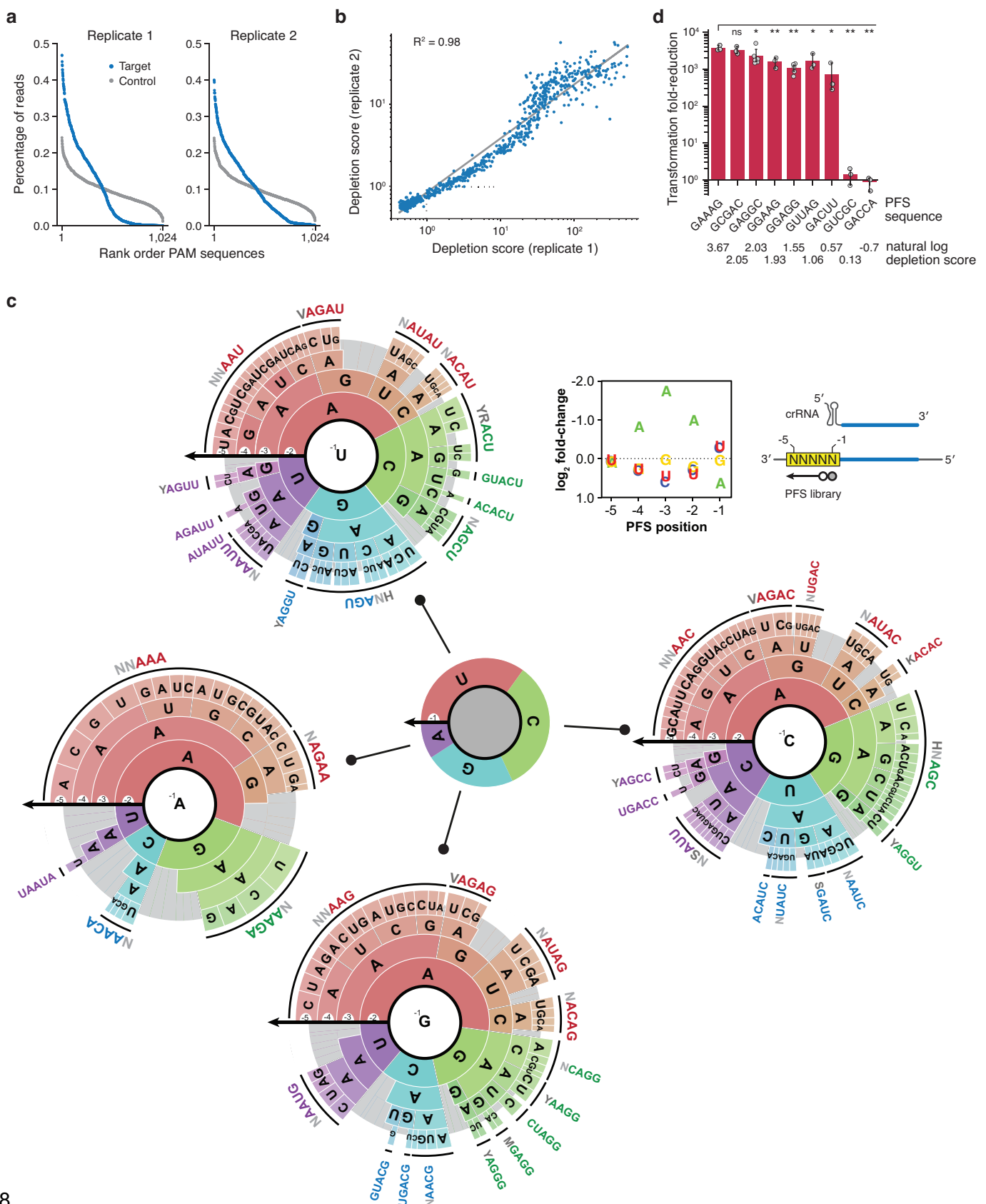
1050 **Extended Data Figure 8 |** Cas12a and Cas12a2 can swap crRNA repeats. The indicated
1051 nuclease, repeat-encoding crRNA, and target were subjected to the traditional (left) and modified
1052 (right) plasmid interference assay in *E. coli*. Bar heights represent mean values from at least three
1053 independent experiments.



1054

Extended Data Figure 9 | Properties of target recognition and collateral cleavage by SuCas12a2.
 (a) Non-specific collateral activities of SuCas12a2, LbCas12a, LwCas13a, and AbCas12g towards FAM-labeled non-target ssDNA, dsDNA, and RNA in the presence of target ssDNA, dsDNA, and RNA. All cleavage reactions were conducted at 37°C unless specified otherwise. AbCas12g was triggered by RNA and ssDNA, and it exhibited preferential collateral cleavage of RNA over ssDNA but no discernable cleavage of dsDNA. (b) SuCas12a2-mediated cleavage over time of FAM-labeled RNA (top), ssDNA (middle), and dsDNA (bottom) non-target substrates. These substrates are cleaved by SuCas12a2 through its non-specific collateral activity. (c) Electromobility shift assay indicating SuCas12a2 and LbCas13a do not indiscriminately degrade dsRNA. Uncleaved substrates and cleaved products are indicated. (d) Impact of mutating

1065 conserved cysteines within the predicted Zinc finger domain of SuCas12a2 on RNA-triggered
1066 collateral activity. The mutated cysteines within SuCas12a2 are C1170S, C1173S, C1188S and
1067 C1191S.

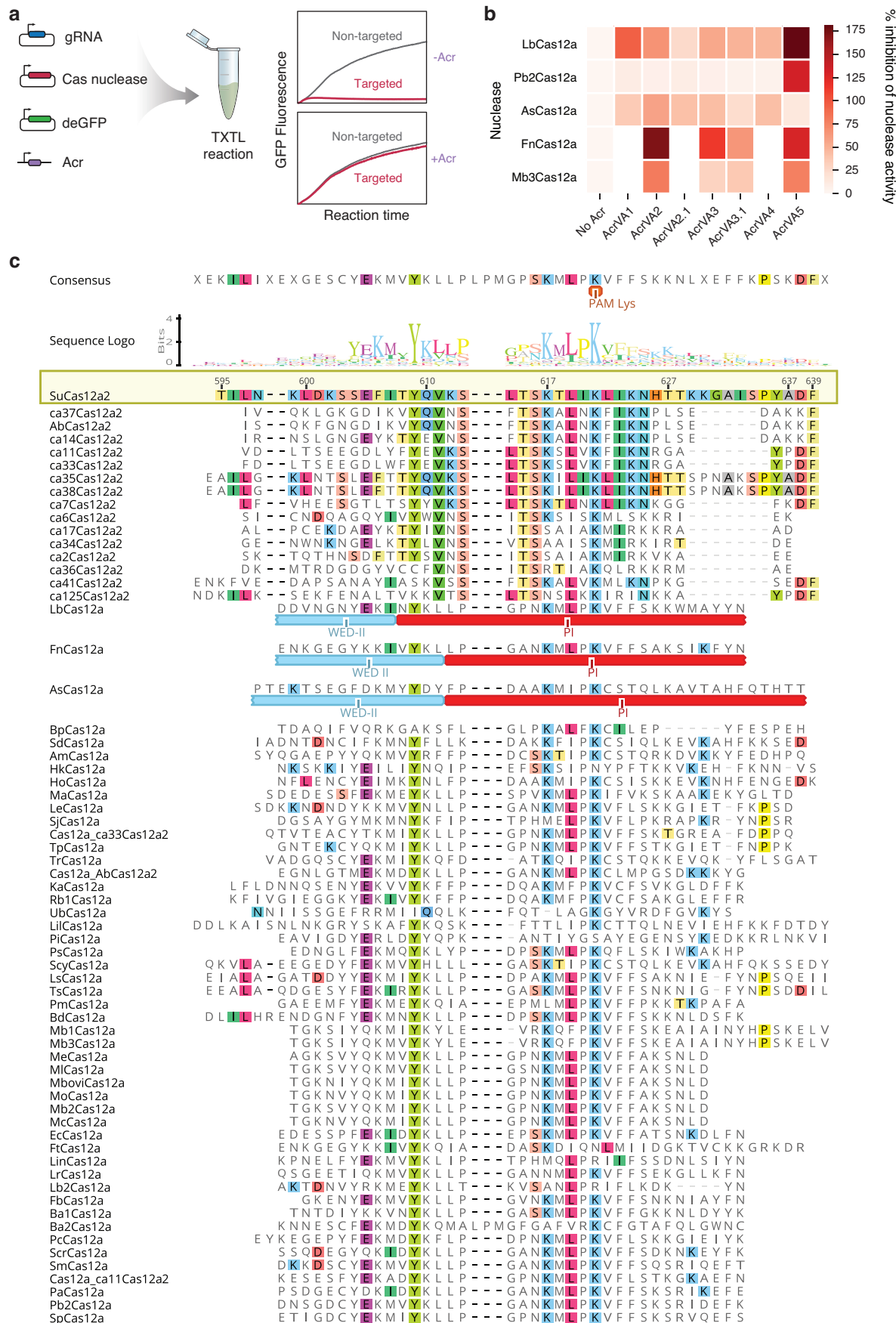


1069 **Extended Data Figure 10 |** PFS depletion screen with SuCas12a2 in *E. coli* BL21(AI). **(a)**
1070 Sequencing coverage of the PFS libraries from the target and the control *E. coli* cultures. Data
1071 from two biological replicates are shown. **(b)** Correlation between the depletion scores obtained
1072 from the two replicate libraries. **(c)** The complex PFS profile recognized by SuCas12a2. See (ref.
1073 ⁶²) for more information on interpreting PAM wheels. Given the complexity of the PFS profile, four
1074 different PAM wheels are shown based on each nucleotide at the -1 PFS position. **(d)** Validation
1075 of selected PFS sequences identified in the PFS screen with SuCas12a2. Bar heights represent
1076 mean values of at least three independent experiments. Error bars depict one standard deviation
1077 from the mean. Significance was calculated using Welch's t-test (* - p < 0.05, ** - p < 0.005).

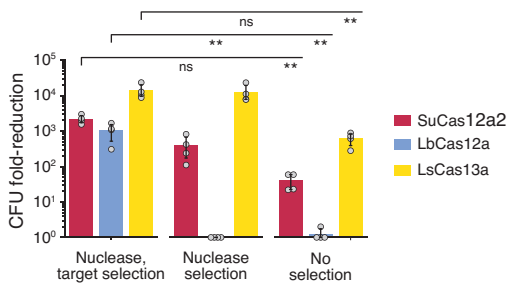
1078

1079 **Extended Data Figure 11 | Impact of SuCas12a2 guide length on plasmid targeting in *E. coli***
1080 BL21(AI). The guide sequence is depicted with blue letters. The standard crRNA guide length
1081 based on crRNA processing (**Extended Data Fig. 7**) is 24 nts. Bar heights represent mean values
1082 from at least three independent experiments. Error bars depict one standard deviation from the
1083 mean. Significance was calculated using Welch's t-test (* - $p < 0.05$, ** - $p < 0.005$).





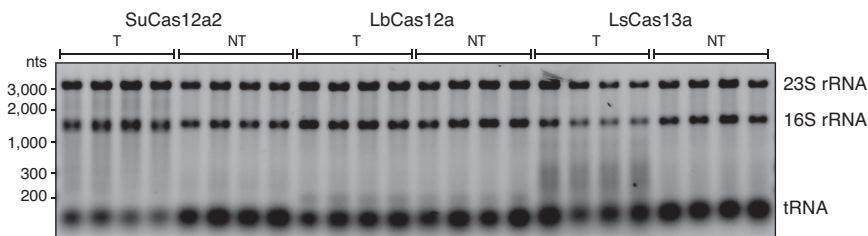
1085 **Extended Data Figure 12 | Verification of DNA targeting inhibition by AcrVA proteins in TXTL.**
1086 **(a)** Schematic of the Acr targeting inhibition assay in TXTL. **(b)** Percent inhibition of Cas12a
1087 activity by the known type V-A anti-CRISPR proteins in TXTL. Inhibition above 100% reflects
1088 higher GFP levels for the target versus the non-target reaction in the presence of a given Acr.
1089 The mean of at least three biological replicates are shown. **(c)** Amino-acid sequence alignment
1090 of the locus containing the lysine residue acetylated by AcrVA5 in Cas12a⁴¹. The alignment shows
1091 that this residue is also present in Cas12a2 orthologs. The highlighted residues represent
1092 conserved amino acids relative to SuCas12a2. Numbering is shown in relation to SuCas12a2.
1093 The domains in FnCas12a⁶⁴, LbCas12a⁶⁵, and AsCas12a⁶⁶ are based on crystal structures.



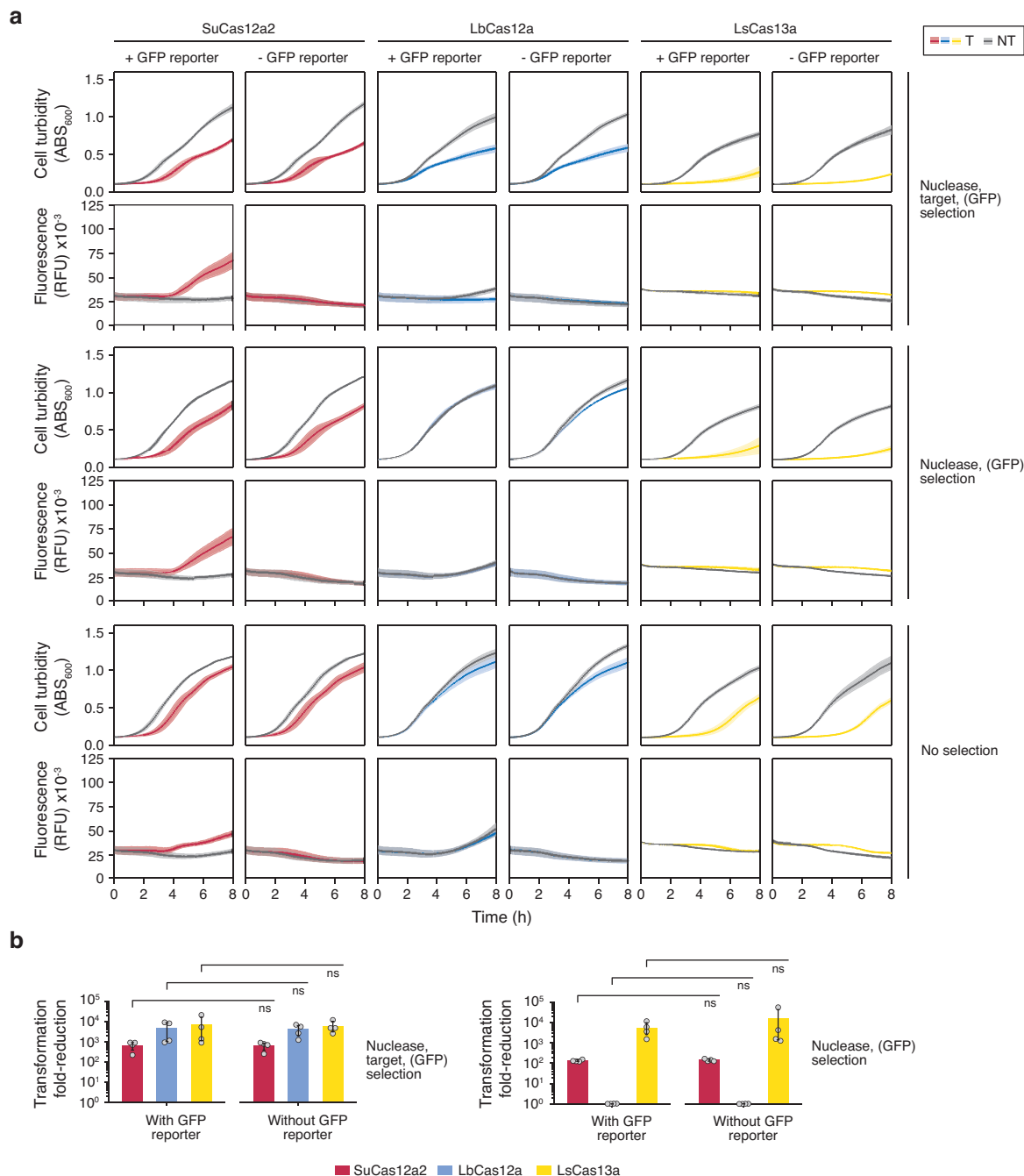
1094

1095 **Extended Data Figure 13 |** Reduction in colony-forming units (CFU) following nuclease and
1096 crRNA induction under different antibiotic selection conditions in *E. coli* BL21(AI). Bar heights
1097 represent mean values of at least three independent experiments. Error bars depict one standard
1098 deviation from the mean. Significance was calculated using Welch's t-test (* - $p < 0.05$, ** - $p <$
1099 0.005).

1100

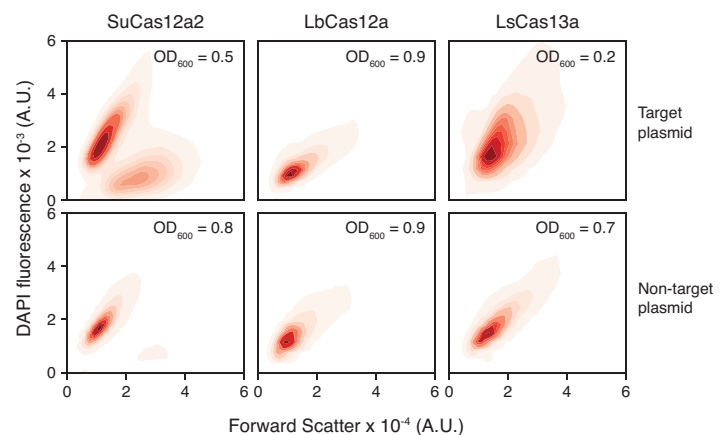


1101 **Extended Data Figure 14 |** SuCas12a2 nuclease degrades cellular RNA. 1% agarose gel shows
1102 total RNA extracted with *E. coli* BL21(AI) expressing SuCas12a2, LbCas12a and LsCas13a under
1103 target (T) and non-target (NT) conditions. Expression of the nucleases and crRNA was induced
1104 with 10 nM IPTG and 0.2% arabinose for 2 hours. Individual wells for each condition represent
1105 biological replicates. Nucleotide sizes are based on a resolved RNA ladder.



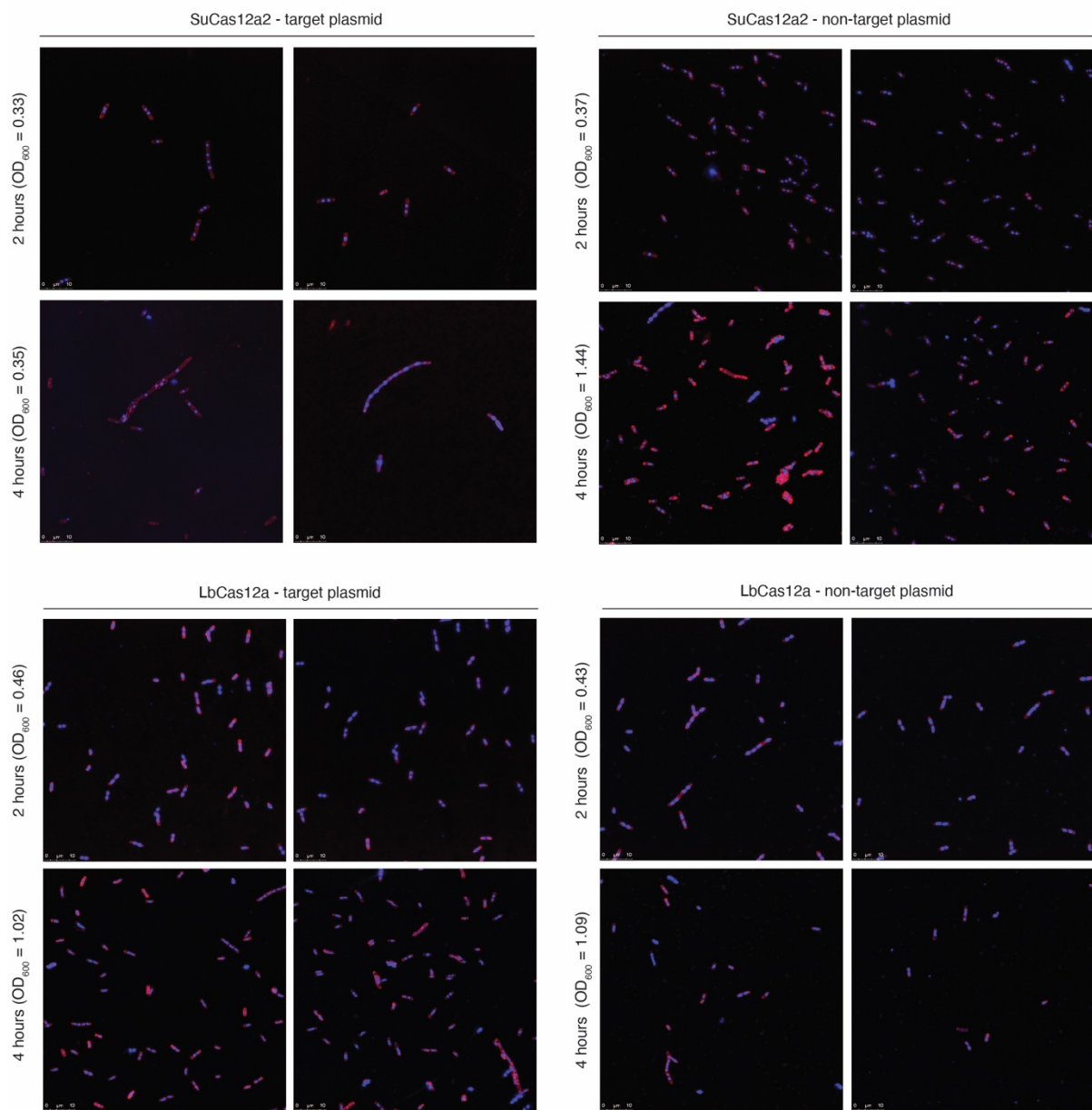
1106

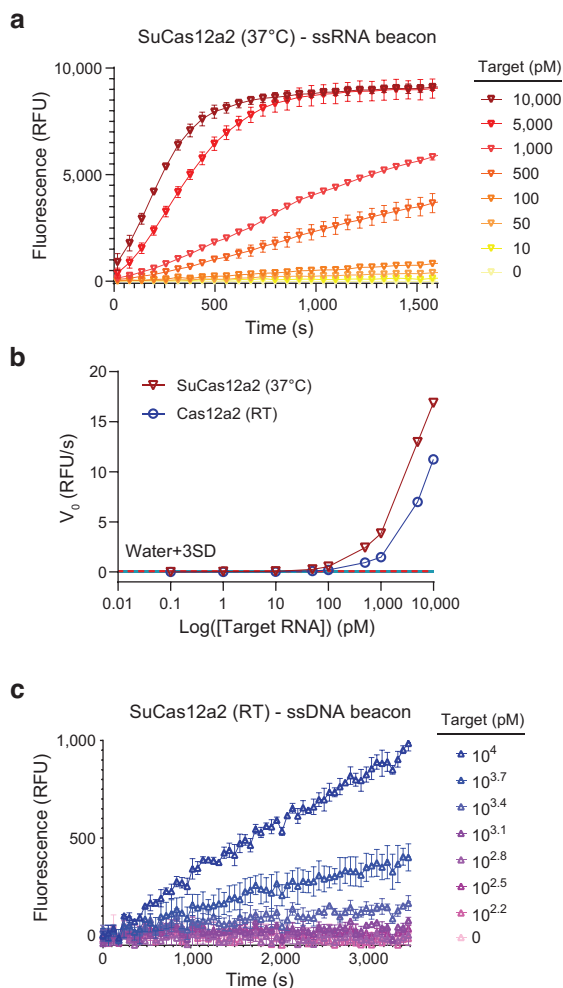
1107 **Extended Data Figure 15 |** Inclusion of the SOS reporter construct does not perturb plasmid
1108 interference by the different Cas nucleases. **(a)** Turbidity and fluorescence time course
1109 measurements when assessing the SOS-responsive GFP reporter under different antibiotic
1110 selection conditions in *E. coli* BL21(AI). Darker bands represent the mean values of four
1111 independent experiments. The shaded areas depict one standard deviation from the mean. **(b)**
1112 Impact of the SOS-responsive GFP reporter on plasmid interference in *E. coli* BL21(AI) under
1113 different selection conditions. Bar heights represent mean values of four independent
1114 experiments. Error bars depict one standard deviation from the mean. Significance was calculated
1115 using Welch's t-test (* - $p < 0.05$, ** - $p < 0.005$).



1116

1117 **Extended Data Figure 16** | Flow cytometry analysis of the nuclease-expressing *E. coli* cells
1118 without antibiotic selection. The cultures were collected four hours after inoculation and induction
1119 of nuclease and crRNA. Prior to the analysis, the cells were stained with DAPI. The subpopulation
1120 with low DAPI and high forward scatter reflects elongated cells with reduced DNA content.
1121 Contour plots are representative of four independent experiments.





1130

1131 **Extended Data Figure 18 |** Determination of the limit of detection by Cas12a2 by velocity
1132 method¹⁸. (a) Progress curve for RNA activated cleavage of RNA beacon by Cas12a2 at 37°C.
1133 (b) Limit of detection of Cas12a2 using RNA beacon was determined using the velocity method.
1134 Velocities were obtained by regression analysis of the linear regions of the progress curves. The
1135 velocity method was used to determine all reported limits of detection. (c) Progress curve for RNA
1136 activated cleavage of ssDNA beacon by Cas12a2 at ambient temperature (RT).

1137 **EXTENDED DATA TABLES**

1138

1139 **Extended Data Table 1** | Tabular data. See the Extended Data Table 1.xlsx file.

1140 - Tab 1: List of strains used in this work.

1141 - Tab 2: List of plasmids used in this work.

1142 - Tab 3: List of key oligonucleotides, synthetic RNA, and dsDNA used in this work.

1143

1144 **EXTENDED DATA FILES**

1145

1146 **Extended Data File 1** | Fasta file listing Cas12a2 and other type V nucleases.